UNIVERSITÀ DEGLI STUDI DI PADOVA

DIPARTIMENTO DI INGEGNERIA INDUSTRIALE

CORSO DI LAUREA MAGISTRALE IN CHEMICAL AND PROCESS ENGINEERING

Master's Degree Thesis in Chemical and Process Engineering

Enhancing the understanding of furfural oxidation: mechanistic insights and kinetic modelling of a heterogeneous catalytic reaction

Relatore: Prof. Paolo Canu

Correlatori: Prof. Tapio Salmi, Prof. Dmitry Murzin, Prof. Johan Wärnå

Laureando: Enrico Marchi

ANNO ACCADEMICO 2022 – 2023

Abstract

This Thesis work has been performed at Åbo Akademi University in Turku, Finland, under the guidance and support of Prof. Tapio Salmi, Prof. Dmitry Murzin, Prof. Johan Wärnå, Prof. Paolo Canu and the supervisor Dr Wander Perez Sena.

This master's thesis aimed to study the mechanism and kinetics of the oxidation reaction of a bio-based compound in the presence of a heterogeneous catalyst, to prepare useful industrial chemicals. In particular, the reaction of furfural with hydrogen peroxide was investigated on a sulfonic resin (Amberlyst-15), in an aqueous phase. The main products of interest were succinic and maleic acids, which are mainly used in the polymer industry, but also for surface coatings, additives, plasticizers, drugs, food supplements and dyes.

Experiments were carried out in an externally recycled packed bed reactor, with a mixing tank in the recycle loop. Each experiment operated at full recycle for several hours, with different operating conditions to investigate the kinetics. The composition was monitored by HPLC.

Experiments feeding the intermediates allowed us to understand the paths in the reaction network towards the products, and later to identify the actual intermediates responsible for the formation of the main product, succinic acid.

The residence time distribution tests were performed with a UV absorbing dye to understand the flow pattern in the reactor, and to estimate the axial dispersion coefficients used in the balance equations for the packed bed.

An improved reaction mechanism compared to the literature was proposed, which describes the concentration profiles and the origin of the main compounds and presents the intermediate molecule for the synthesis of succinic acid. A total of 50 parameters, including 25 for the activation energy, 25 pre-exponential constants were used in the mathematical model to describe all the reactions. The best-fit parameters have been determined by comparing multiple experiments with the predictions of a reactor model, numerically solved by an original MatLab script. The axial dispersion model was solved by discretizing the length of the reactor using the backward finite difference method.
The optimization was based on the objective function calculated as the average of the square difference of calculated and experimental concentrations.

Finally, sensitivity analysis was performed, showing the statistical significance of the final parameters.

Table of contents

Introduction

Since the increasingly growing alarm towards global warming, pollution and resource scarcity, the attention in the chemical industry is progressively focused in developing alternative ways to synthesize useful chemicals, in order to reduce the use of petrochemicals derivatives [1].

The chemical industry, being a significant contributor to global emissions and waste, has witnessed a shift towards eco-friendly alternatives. An example of sustainable solutions lies in the utilization of wood-based molecules, which offer an immense potential for transforming the chemical industry while mitigating its environmental impact. Since wood is one of the most abundant natural resources, many countries, and particularly in Finland, are investing on the development of processes, which use wood derived compounds [2].

The *Green* offer of wood-based molecules makes it an attractive solution from many points of view:

Sustainability: The production of wood-based molecules involves harnessing the power of photosynthesis, a natural process that consumes carbon dioxide and releases oxygen, which creates a circular economy, making it a sustainable alternative to fossil fuels.

Low carbon footprint: When compared with traditional petrochemicals processes, wood-based molecules have a significantly lower carbon footprint. By using wood and other vegetable waste as a feedstock, the industry can reduce the greenhouse gas emissions and contribute to the battle against climate change.

Abundance and renewability: Forests covers nearly 31% of the Earth's land area, making wood-based molecules readily available while originated from a renewable source. This can be applied in combination with a responsible forest management to ensure a continuous supply of the raw material, avoiding depletion.

Diverse applications: Wood-based molecules can be transformed into a wide range of products, including biofuels, bioplastics, pharmaceuticals, and speciality chemicals.

Recent advancements in green technology have brought the development of processes which are able to transform the raw renewable feedstock to various commodity, speciality, and fine chemicals. Innovations of homogeneous and heterogeneous catalysts, enzymes and processes have facilitated the efficient conversion of lignocellulosic biomass, from complex structures to simple sugar monomers which are used as building blocks. Such wood-based molecules can produce biofuels as already available in the market, for example bioethanol, biodiesel, and green-diesel, allowing a balance between the CO_2 emitted and the one used by plants [3].

A great innovation, which is an attractive field of current research, is the development of biodegradable and compostable bioplastics from renewable sources, which can become a solution to the pollution of non-degradable plastics all around the world.

In the laboratory where this thesis has been elaborated, the main focus is on the development, use and evaluation of heterogeneous catalysts in chemical transformations.

This master's degree project had the aim to investigate a possibility to produce valuable components such as succinic and maleic acids from a renewable material, in this case: furfural using Amberlyst-15, a polymeric acidic catalyst. This is part of a broader research effort where wood and plant leftovers are processed and reacted into molecules useful for the industry.

Previous studies of furfural oxidation on heterogeneous catalysts have been conducted to understand the reaction mechanism, catalysts activity and to produce valuable molecules. The reaction mechanism initially considered for this project was presented previously in the literature [4], where an acidic catalyst was investigated, and it is displayed in Figure 1.

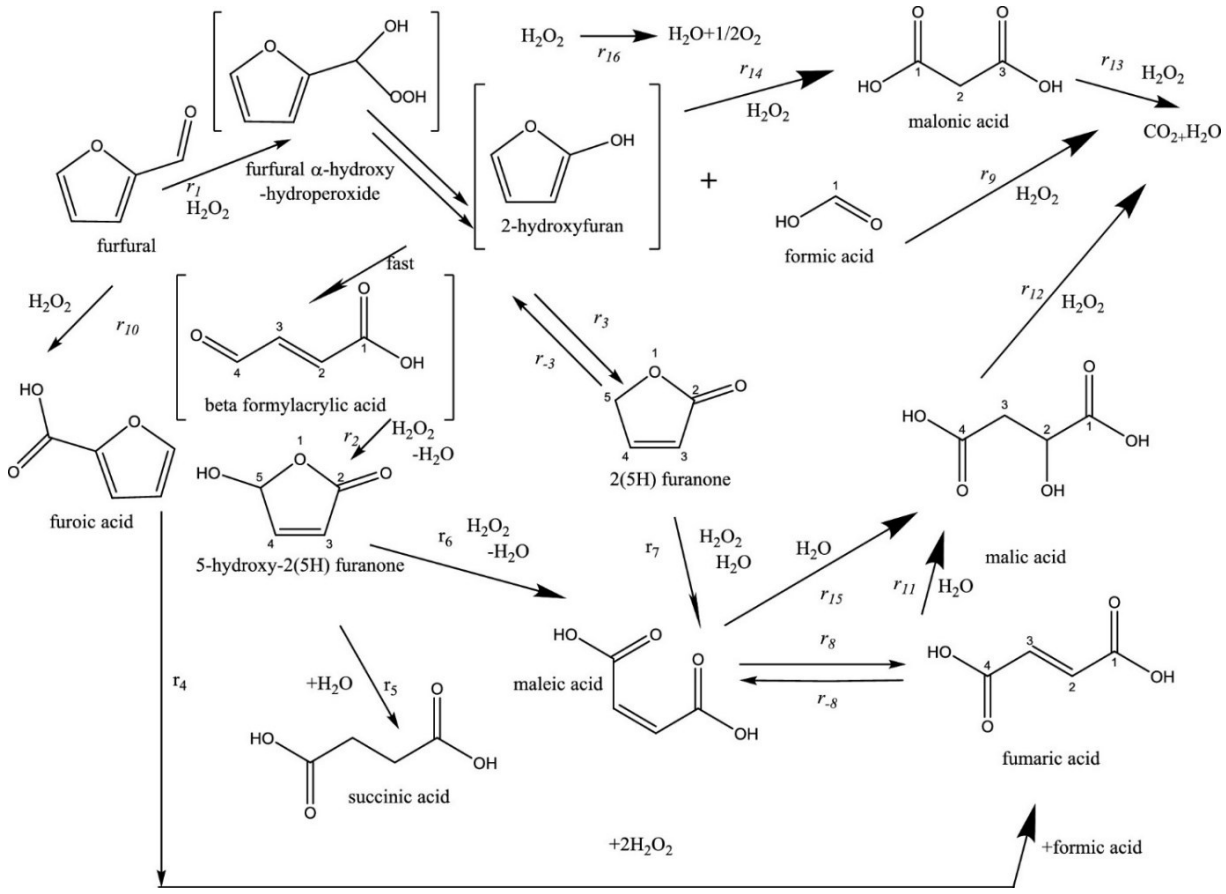

Figure 1. Reaction network for furfural oxidation with hydrogen peroxide over sulphated zirconia [4].

The use of hydrogen peroxide proved to be an efficient liquid oxidizer of organic compounds and specifically for furfural, accordingly to many authors [4-5-6-7].

The reaction network shown in Figure 1 represents the starting point for the drawing of a new mechanism, where some variations were introduced after the results of the experiments with the reaction intermediates.

Other authors [8-9], have briefly studied many different catalysts to be applied on furfural oxidation, among them, Amberlyst-15 has shown interesting results.

With this study, the aim was to investigate the oxidation of furfural on Amberlyst-15 to highlight the best operating conditions. In addition, a better understanding of the reaction network was required to explain the consumption and appearance of the main compounds present in the reaction medium. Finally, there was the interest to understand if a packed bed reactor operated at full recycle mode could offer a promising solution to conduct slow reactions. Such a setup can be useful in case scale-up.

In the first part of this thesis an overview is provided on the main compounds involved in the reaction system with their significant properties, market shares and applications.

Then a description of the equipment used to carry out the experiments and the techniques applied to analyse the samples are presented, followed by a description of the catalyst and the residence time distribution measurements in the packed bed reactor.

The experiments with the initial substrate and various intermediates are presented, resulting in developing the reaction network, more detailed than discussed in the literature.

Finally, the derivation of kinetic equations, the data fitting, and the results are described. In the end, few plots of the calculated concentration profiles and the experimental points along with the statistical analyses of the estimated parameters are displayed.

CHAPTER 1
EXPERIMENTAL METHODS

1.1 Objective of the study

The objective was to investigate the reaction mechanism involved in the catalytic oxidation of furfural, a bio-based molecule, with hydrogen peroxide. This was necessary to understand if the reactor setup, described later, would offer an improvement compared to a classical batch or semi-batch technology, and to better explain the reaction mechanism. The two products of interests were succinic and maleic acids. A set of experiments at different conditions has been performed and further used for kinetic modelling to determine the kinetic constants and the activation energies of all the reactions involved.

1.2 Main chemicals involved in the reaction system

The two reactants used in this process were furfural and hydrogen peroxide, which react on a polymeric resin catalyst Amberlyst-15 with strong acidic properties. From the primary reaction, unstable and stable intermediate compounds are formed, finally yielding desired and undesired products.

1.2.1 Furfural

Furfural (Figure 1), an organic compound obtained mainly from the monomeric sugar xylose, can be used as a precursor to the synthesis of useful molecules for chemical industry. Among many applications of its derivatives, production of solvents, fuel additives, polymerization monomers and molecules for pharmaceutical synthesis can be mentioned. Furfural is a toxic, irritant, and carcinogenic compound which is flammable at temperatures exceeding 60°C. Furfural in its pure form is an oily colourless liquid, even though self-polymerization gives it a reddish-brown tint, and it is characterized by a pungent sweet-cinnamon-almond like smell [10].

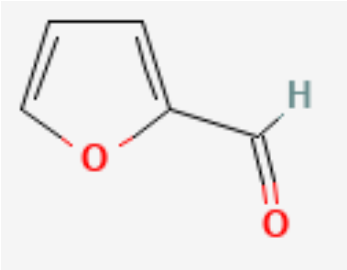

Figure 1. Furfural.

Some of the most important physical properties of furfural are reported in Table 1.

Table 1. Main physical properties of furfural.

T melting	***T boiling***	***Flash point***	***Density***	***Solubility in water at 20°C***	***Vapor pressure at 20°C***	***Viscosity at 25°C***
-38.1°C	162°C	60°C	1.16 g/cm^3	8.3 g/100mL	2.21 mmHg	1.587 mPa*s

Bio-based furfural is mainly obtained from corn stover and corn cobs and also from other agricultural wastes which are by-products of the plants not used in food production. The main reactions involved in the furfural production are hydrolysis of hemicellulose into monomeric sugar molecules (xylose) and the dehydration of sugars into furfural [11]. Since it originates from a renewable source, it is nowadays of a great interest to understand and develop processes, which uses this molecule to synthesise valuable organic compounds.

Furfural is considered one of the top 30 platform chemicals and in 2021 it was produced with a global volume of 348 kt, valued at ca 560 million USD. It is believed that the value of furfural will increase with an annual growth rate of ca 7% (between 2023 and 2030) as the world is pushing towards more renewable processes [12]. In 2021, most of furfural was produced using small and medium batch processes in China, using agricultural leftovers. Furthermore, among the continents, Asia has currently the highest usage of it with more than 75% of the global production. As for the end-use outlook in 2021, furfural is mainly used in refineries, but also in pharmaceutical, paint, coatings, and agriculture.

1.2.2 Hydrogen peroxide

The second reagent, hydrogen peroxide is a strong oxidant and irritant, and was used in this work because of its ability to oxidize furfural in liquid state. The initial concentration of 30% was applied.

In Table 2 some of the most important physical properties of hydrogen peroxide are shown [13].

Table 2. Main physical properties of hydrogen peroxide.

T melting	***T boiling***	***Density***	***Solubility in water at 20°C***	***Vapor pressure at 25°C***	***Viscosity at 25°C***
-26°C at 30%	107°C at 30%	1.1 g/cm^3	completely soluble	1.97 mmHg	1.819 cP

The global hydrogen peroxide market size was valued at 3.2 billion USD in 2022 and is projected to reach 4 billion USD by 2027, growing at ca 5% from 2022 to 2027. Hydrogen peroxide is essential in the chemical industry for selective oxidations of organic compounds [14].

1.2.3 Succinic acid

The main product of interest from this process is succinic acid (Figure 2), which is obtained along with many other products.

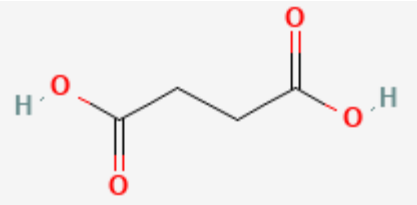

Figure 2. Succinic acid.

Succinic acid is a valuable dicarboxylic acid which can be used as a precursor to polymers (polyesters and polyamides), resins and solvents. Furthermore, it is used as a food supplement, as well as dyes, perfumes, cosmetics, plasticizer, metal treatment, chemicals and coatings [15].

The main physical properties of succinic acid are shown below in Table 3.

Table 3. Main physical properties of succinic acid.

T melting	***T boiling***	***Flash point***	***Density***	***Solubility in water at 25°C***
188°C	235°C	206°C	1.1 g/cm^3	8.32 g/100mL

Succinic acid is currently produced in chemical industry using crude oil as feedstock, and it had a market size of 2.4 million metric tons in 2021, valued at 223 million USD. It is believed that its value will increase with an annual growth rate of ca 10% (from 2022 to 2030). The two most important geographic areas for the consumption of succinic acid are Asia-Pacific and North America [16].

1.2.4 Maleic acid

Maleic acid (Figure 3) is a colourless, crystalline organic dicarboxylic acid. It is combustible, although difficult to ignite, and it is considered toxic, causing extreme irritation to eyes, skin, and respiratory systems.

Maleic acid is the second product of interest from the catalytic oxidation of furfural.

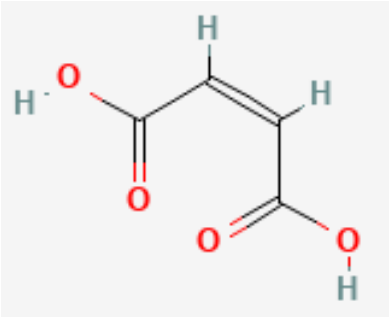

Figure 3. Maleic acid.

Maleic acid is used to make alkyd and polyester resins, surface coatings, lubricant additives, plasticizers, adhesives, copolymers, drugs, and agricultural chemicals. It is also used to retard the rancidity of oils and to dye and finish textiles (wool, cotton, and silk) [17].

The main chemical properties of maleic acid are shown in Table 4.

Table 4. Main physical properties of maleic acid.

T melting	***T boiling***	***Flash point***	***Density***	***Solubility in water at 25°C***	***Vapor pressure at 20°C***	***Decomposition T***
130.5°C	355°C	127°C	1.59 *g/cm^3*	788 g/L	0.0000359 mmHg	135°C

The global malic acid market size was valued at USD 216.21 million in 2022 and is projected to grow at an annual growth rate (CAGR) of ca 5% from 2023 to 2030 [18].

1.2.5 Materials

Furfural (≥98 wt%), fumaric acid (≥99 wt%), succinic acid (≥99 wt%), 2-furoic acid (98 wt%), 2(5H)-furanone (98wt%), maleic acid (≥98 wt%), hydrogen peroxide (30 wt%) were purchased from Sigma Aldrich, formic acid (98 wt%) was supplied by J.T. Baker, malic acid (99%) from Acros Organics and malonic acid (99%) from Merck.

1.3 Reactor setup and equipment used for the experiments

The experimental system consisted of a well-mixed vessel followed by a packed bed reactor, operated at a full recycle mode. The reactor setup used to perform the experiments, shown in Figure 5, was used instead of a simple batch reactor because there was an interest to understand if a packed bed reactor operating at complete recycle might improve the yield of succinic acid. For slow reactions, this kind of setup could prove to be useful since it is used with full recycle or a high ratio of recycle over the outlet. In this way, small amounts of catalyst are placed in the packed bed

reactor, and it is continuously crossed by the reacting mixture. Faster production can be reached by adding more catalyst per unit volume or by increasing the length of the reactor bed.

Furthermore, such reactor offers a fixed deal of the solid catalyst, which stays in place during the whole reaction time, while in a batch reactor, the vigorous mixing leads to impacts between the particles and the stirrer. Intense stirring can cause friction and mechanical destruction of the catalyst beads. Finally, the catalyst loading can be higher and separation of the reaction mixture in a PBR is easy, contrary to the batch operation when filtration is necessary.

This kind of reactor setup helps to understand the difficulties and differences in the shift from batch to continuous processes in scale up.

The equipment used for the experiment was composed of a jacketed mixed tank with a nominal volume of 250 ml with four openings at the top and one in the bottom for the exit of the process mixture plus two on the side for the jacket. At the top, a condenser is used to prevent water from evaporating and consequently changing the concentration. The second opening was used as an inlet of the recycled mixture coming from the PBR column; one opening was used to pour the solutions and for sampling through a thin tube. The last one had a thermocouple going in the vessel to track temperature variations in the mixing vessel. The bottom outlet was connected to a peristaltic pump with a rubber pipe. The mixture was sent in the up-flow mode to the packed bed reactor.

The reactor was composed by three areas. The first one, at the bottom, was filled with small glass spheres, supporting the packing above and uniformly distributing the mixture. Above, a mixture of catalyst particles and the glass spheres were placed with a ratio of 1/10, which is necessary as the catalyst swells in the solution, subsequently with a high volume of inert it was possible maintain the flow. In the middle of this catalytic bed a thermocouple was placed to carefully adjust the temperature to the desired value. The uppermost area was composed only of glass spheres, allowing efficient mixing before returning back to the stirred tank.

The peristaltic pump had the possibility to vary the range between 15 and 200 ml/min. The stirring into the mixing vessel was kept at 700 rpm. The heating water, whose temperature was adjusted electronically, flowed in the system first entering into the packed column jacket and then in the jacket of the mixing tank. The cooling water, tinted with a light blue (Figure 4), was recirculated in a coil where water condensed but light gases such as CO_2 or O_2 can escape, avoiding any pressure increase in the system.

The two green wires were connected to the thermocouples, connected to a computer which stored the temperature profile and adjusted the heating water temperature in real time. A chronometer was used to check the reaction time and to precisely define the sampling moments. A manometer was also added at the bottom of the glass column to check any unexpected pressure increase. If this is the case, it indicates a clogging in the reactor, which could cause leaking from the glass connections or silicon-glass connections.

Aside of this equipment vials for the sampling collection are placed in a vial holder, with a special notation to identify a particular sample.

In figure 4, the reactor setup used for the experiments is shown, while the scheme of such apparatus is shown in Figure 5.

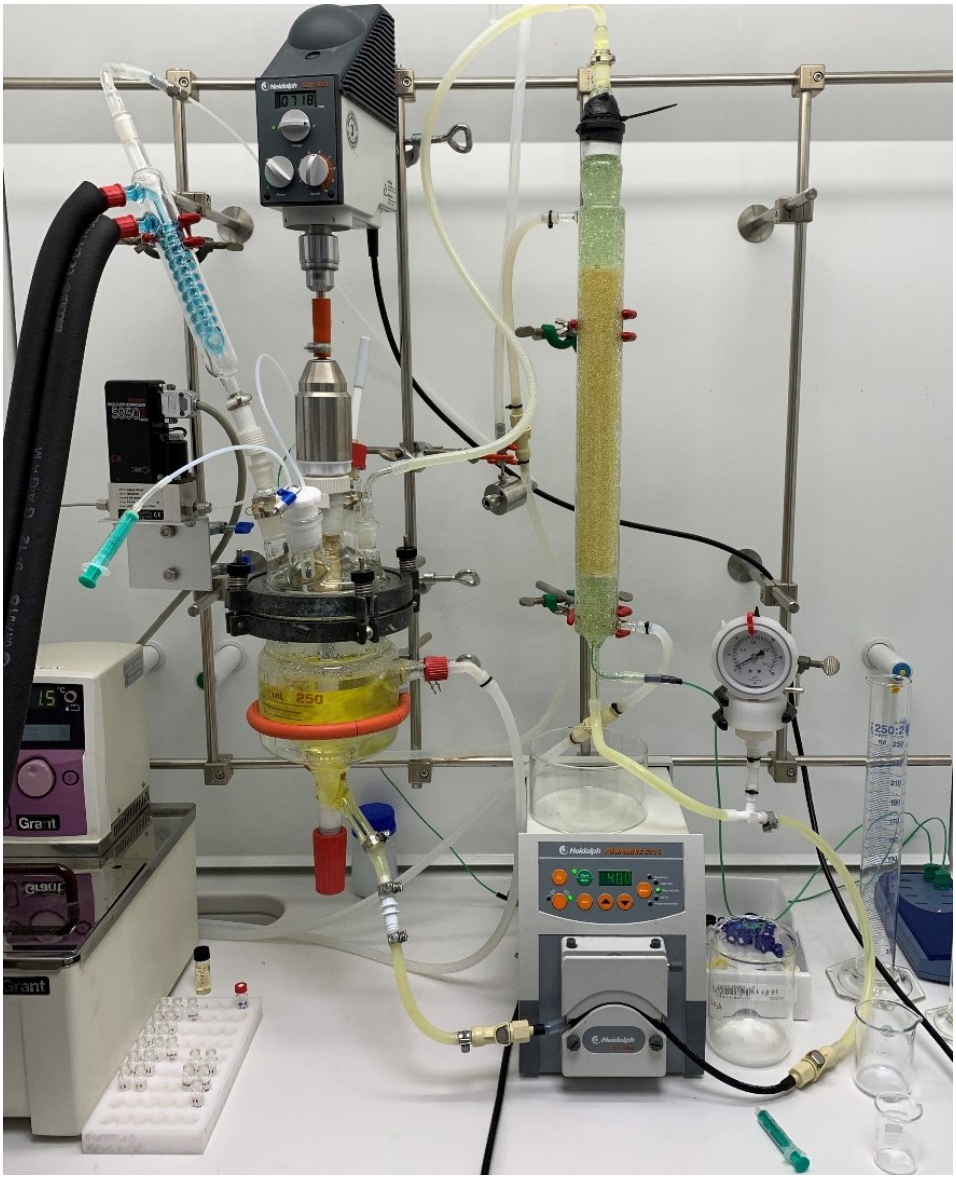

Figure 4. Reactor setup.

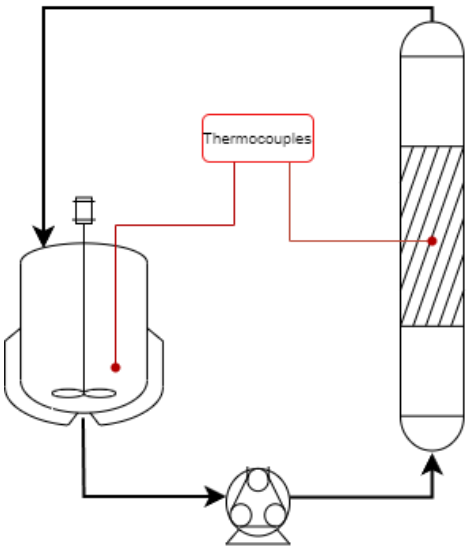

Figure 5. Reactor setup scheme.

1.4 Experimental procedure

Prior to each experiment, the conditions of the apparatus have been checked, particularly the packing, the silicon tubes and the clamps.

In a glass reactor used initially, the catalyst particles moved upwards ending at the top of the active area, creating inhomogeneity. The cause of this unpleasant phenomena was an insufficiently pressed packing in the column, leading to separation from the inert material under the flow of liquid.

Once the equipment was checked, the heating and cooling water systems were turned on. When the stirring tank and the reactor reached the operating temperature, a volume of the furfural solution prepared in advance was poured in the stirred tank, hydrogen peroxide solution of 30% was measured, and mixed with the furfural solution as soon as it reached 75-80°C. After such addition, the temperature was slightly decreased, and mixing occurred for few seconds. Then the bottom exit of the stirred tank was opened, and the pump was turned on. As soon as the liquid level reached the bottom of the catalyst bed, the timer was started, and samples were withdrawn at regular intervals.

Among the two sampling points, the first one was placed inside the stirred tank while the other one was located at the top of the packed bed reactor. Most of the experiments lasted seven hours, while one experiment was conducted for 24 h.

1.5 Analysis of samples

Two syringes were used to withdraw small volumes of the liquid. Each time, before sampling, a withdraw with an immediate re-injection was done with the purpose of washing the small channels, in order to get a representative sample. The usual sample volume was about 0.5-1 ml, which was

analysed by high-performance liquid chromatography (HPLC) Agilent 1100 instrument equipped with an Aminex HPX-87H column filled with polystyrene-divinyl-benzene synthetic resin.

According to the applied program, specifying the temperature, the flow rate and the liquid carrier, each sample required 70 minutes to be analysed. As result, a chromatogram of all the components sufficiently separated from each other was obtained. A dilute solution of sulfuric acid at 5mM was used as a mobile phase. The analysis was performed at 90 bar and 55°C.

The analysis of the samples with the HPLC were performed by an UV lamp, which continuously irradiated the cell at the outlet of the column. If only the mobile phase passed, the light completely went through to the analysis cell; while, when a substance passed through the cell, the light was refracted and caught by the refractive index detector (RID) [19].

At the end, using the software of the HPLC, the areas of each peak were defined manually.

All the known compounds present in the reaction media were analysed individually at different concentrations by HPLC. This was done to identify the retention time at which they will appear in the chromatogram and to correlate the peak areas with the concentrations.

An example of refractive index detector chromatogram is presented in Figure 6:

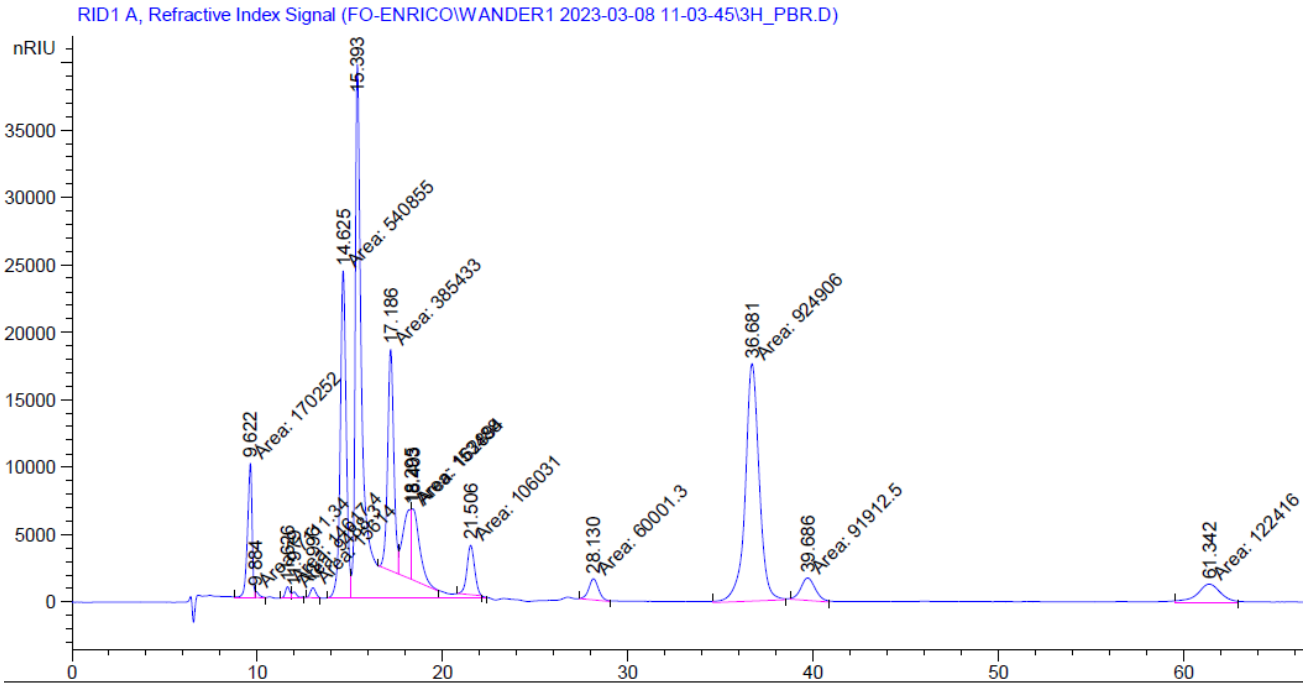

Figure 6. Example of a refractive index chromatogram.

Figure 6 shows an example of the chromatogram illustrating the compounds present in the reaction mechanism after three hours. The most important components in the example are maleic acid (9.6 min), succinic acid (14.6 min), hydrogen peroxide (15.4 min), 2(5H)-furanone (36.6 min), formic acid (17.2 min) and the last one is furfural (61.3 min). For hydrogen peroxide a long tail was noticed, allowing to take it into account while calculating the concentration of compounds with closer retention times.

1.6 Catalysts

1.6.1 Amberlyst-15

The catalyst used was Amberlyst®-15 in H^+ form, which is a Brønsted acidic resin in the form of small spheres made of macroreticular polystyrene-divinylbenzene with sulfonic functional groups attached to it [20]. These resin spheres are characterized by a high porosity with large pore sizes and a surface area of around 53 m^2/g [21]. The catalyst was provided from Sigma-Aldrich (Merck) in a wet state, with the water content of ca 50% wt.

In dry form, the resin has a density of 1.2 g/cm^3 with a brown-grey colour and strong electrostatic behaviour; after being wetted it gains a brownish to pale yellow colour depending on its wetness with the density decreasing to ca 0.75 g/cm^3.

Figure 7 contains some images of the Amberlyst-15.

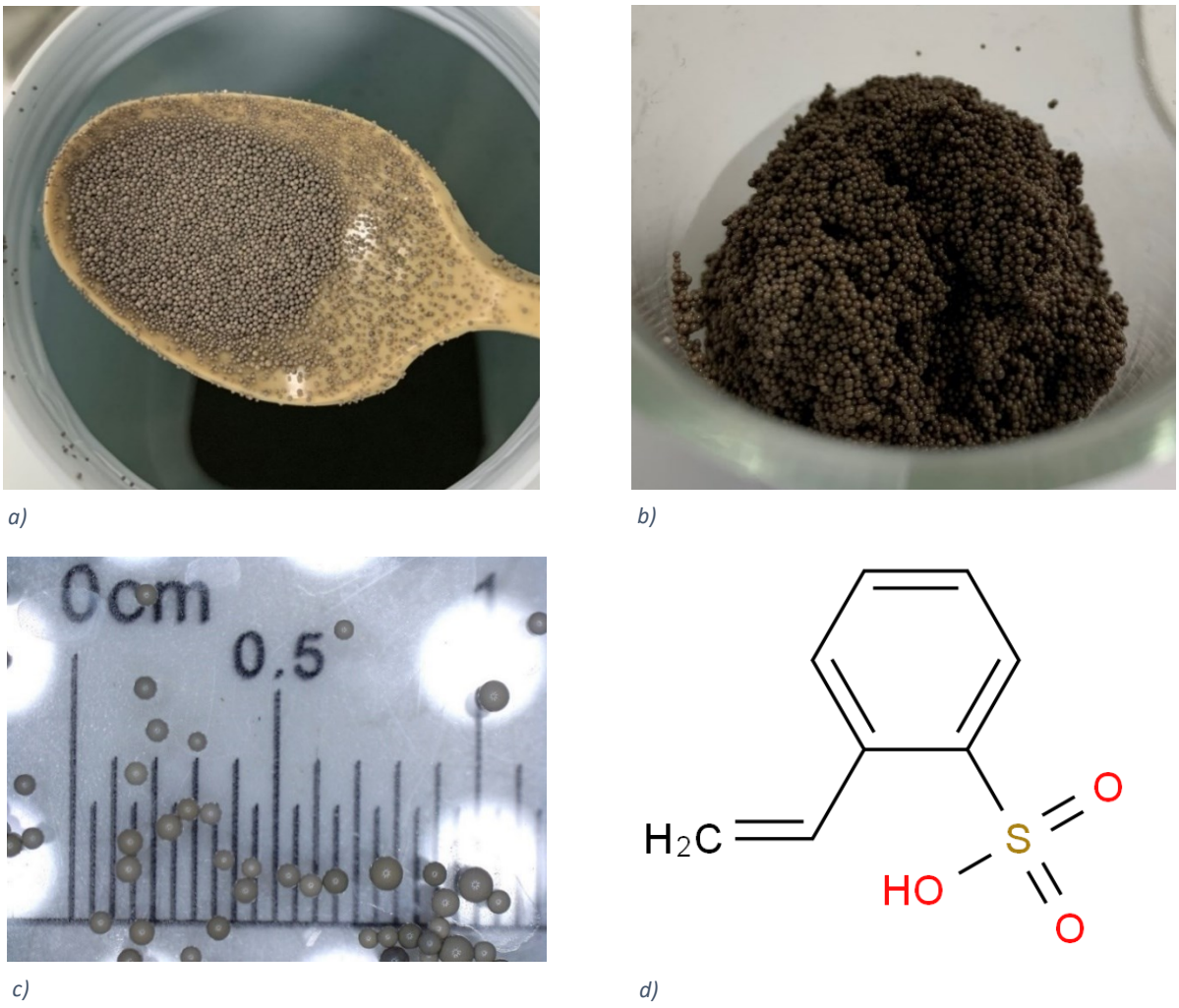

Figure 7. (a) dry, (b) wet, (c) particle size distribution of the wet catalyst, (d) a sulfonic group attached to the styrene molecule of the polymer.

In Figure 8, changes in the polymeric catalyst are shown, depending on the wetting conditions, swelling and exposure to the solvent/reaction mixture. In case of brown colour, there was insufficient swelling. To reach the optimal conditions shown in Figure 9b, it was necessary to circulate water at temperature exceeding 60°C for few hours.

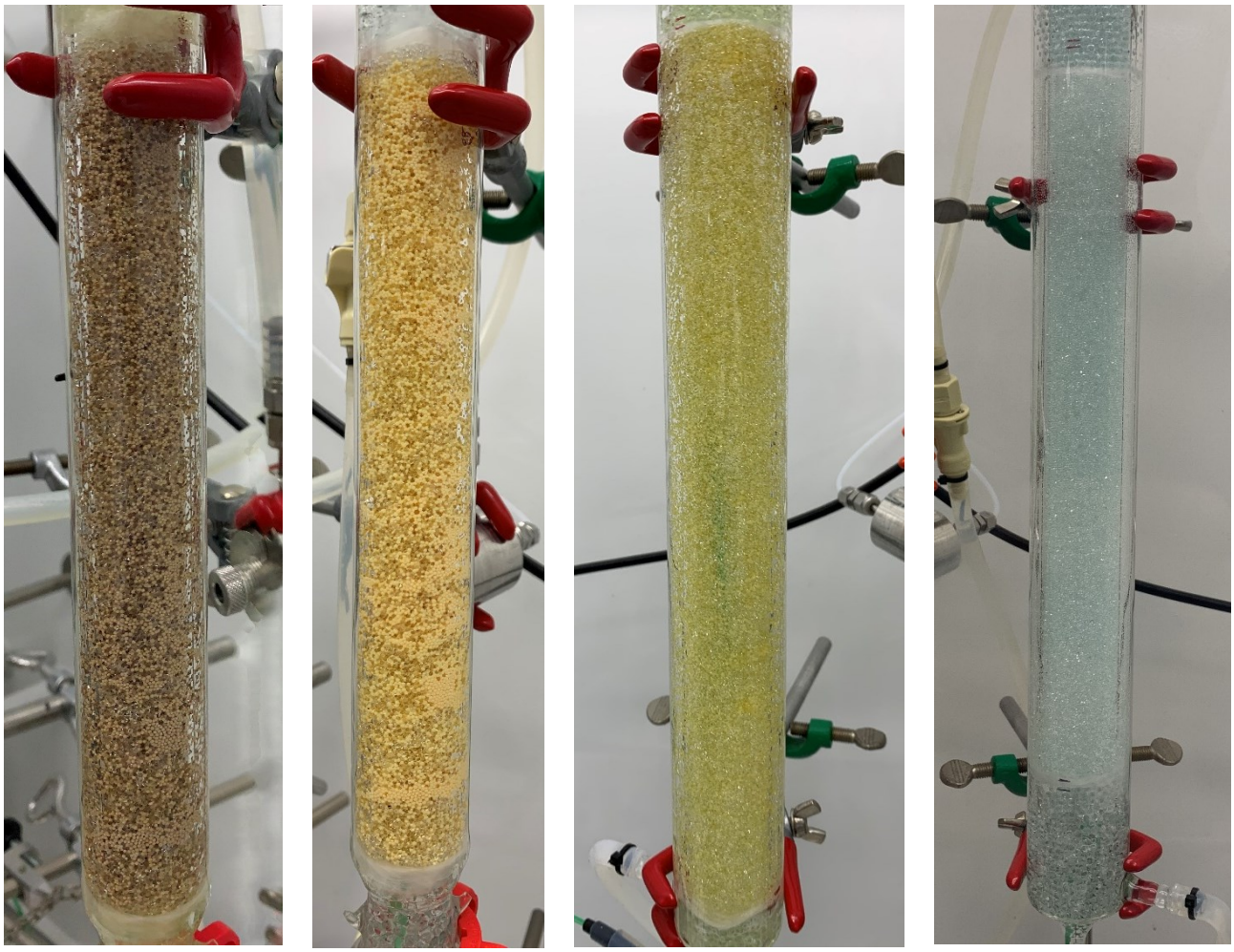

a) *b)* *c)* *d)*

Figure 8, Different swelling stages. (a) the catalyst had been wetted for just one hour with water, (b) after few hours in contact with the solution at 80°C and up to 25-30 hours where the catalyst is considered stable with constant activity. (c), after more than one week of constant wetting with water and the reaction solution. (d) the catalyst has disappeared after two weeks in contact with the solution at high temperature.

After the catalyst had been sufficiently wetted and swelling had stabilized, the tests have been performed.

It was found out that the activity and selectivity towards of desired products was constant for the first three 7 h experiments conducted under identical conditions. After more than 21 h in the acidic and oxidant environment at 80°C, the catalyst started to be paler, and the activity decreased slowly. For this reason, to obtain representative experiments, it was decided to regenerate the catalyst after the

first experiment and discard it after the second one. In this way, the column was packed every second of the 7 h experiments, staying under the 21 h limit.

It was also noticed that the acidic aqueous solution at high temperature (80°C) increased dissolution faster compared to lower temperatures (60-70°C). In another work carried out in the laboratory, the same catalyst was used at 100-110°C in an organic solvent, but in none of the experiments conducted under these conditions, catalyst dissolution was noticed. For this reason, it is assumed that the aqueous solution is essential for the slow disappearance of Amberlyst-15. Because the polymer is not soluble in water or organic solvents, a possible explanation of such a phenomenon is the combination of hydrogen peroxide from the reaction with the sulfonic groups of the catalyst at high temperatures; this will generate peroxymonosulfuric acid, which is one of the strongest oxidizing and corrosive substance, possibly being able to break the polymer bonds.

Another explanation of the catalyst dissolution might be the constant absorption of water in the catalyst which causes swelling of the polymer until the internal pressure breaks the molecular chains in small pieces, which are able to leave from the reactor.

The same type of catalyst with different intramolecular bonds (more reticulated) might behave differently.

1.6.2 Regeneration of Amberlyst-15

Some authors and producers suggest regenerating the resin after few cycles, without being specific about the length of each cycle [22]. According to the catalyst supplier, for the resin regeneration, it is necessary to circulate a solution of 1-5% of sulfuric acid at a low flow rate through the reactor. This is done to restore acidity of the sulfonic groups attached to the polymer resin [23]. For the sake of good performance and repeatability of the results, it was decided to regenerate the resin after each experiment, which usually lasted for seven hours. Because the regeneration continued for five hours, conversion and selectivity of succinic and maleic acid were kept at the same values for the experiments carried out under identical operating conditions.

1.6.3 Packing the reactor column with Amberlyst-15

In the beginning of this project, a 2 cm diameter glass reactor column was used with the catalyst and inert glass spheres in it. After running the first experiment of seven hours, swelling was noticed in the catalyst particles, but the flow continued, and the reaction proceeded with the expected conversion and selectivity. The next day, another experiment of seven hours was started, leading however to a failure. Swelling of the catalyst increased even more, until it was so compact that a jelly-like material was visible in the area, where the catalyst distribution was not homogenous, and the particles agglomerated together. The flow resistance caused a pressure increase at the bottom of the column to

an extent that the bottom joint was detached from the reactor with a leakage of the liquid mixture. This event forced to rethinking of the reactor setup ad its operation mode.

The main problems of this packed bed reactor were that the catalyst was filled with the inert while it was still dry and the ratio of the inert to the catalyst amount was too low. After a proper wetting the catalyst particles increased their size more than twofold diameter, so it was necessary to fill the reactor with an already swollen catalyst.

For the modified reactor setup, few improvements have been implemented with the aim of mitigating the possible blockage of the flow. First of all, the catalyst swollen was used for packing. Another glass column reactor with a larger internal diameter (3 cm instead of 2 cm) was used to diminish the flow velocity. Finally, the catalyst-to-inert weight ratio decreased from 8/80 to 8/310 (g/g). The inert consisted of spherical glass particles with a diameter of 1 mm. In this way a better dispersion of the catalyst was achieved.

The first step when filling the column was to insert a thermocouple in the reactor through a T-joint at 90° angle, where the actual sensor was placed in the centre of the catalyst volume. Glass spheres with 3 mm in diameter were added in the lower part to create a support layer, with few millimetres of wet glass wool to separate the catalyst from falling during the no-flow period. Afterwards, the wet catalyst already well mixed with the glass spheres was added from the top with a spoon. With the help of a wash bottle and two self-made pistons, the catalyst-inert mixture was placed and compacted into position. The first piston has a hole in the centre to slide the thermocouple while pressing and the other one has just flat surface. Figure 11 illustrates the bottom of the two pistons used for packing.

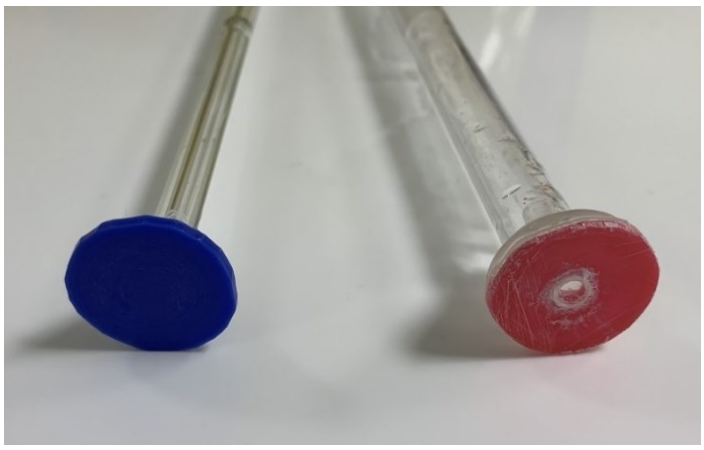

Figure 9. Two custom made pistons to compact the catalyst-glass particles mixture in the reactor.

Just few centimetres of the catalyst-inert were added each time, therefore it was possible with the piston rod to press the active material and remove any possible empty volume which could cause movements, and catalyst particle agglomeration during the experiments and channelling (Figure 10).

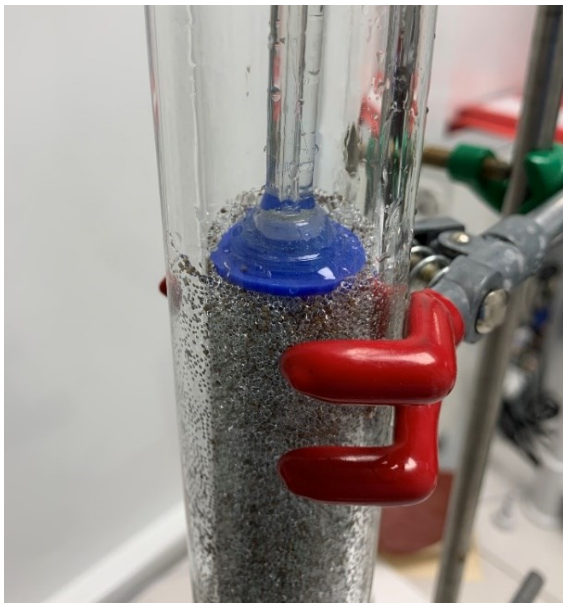

Figure 10. Packing of the column with a mixture of wet Amberlyst-15 and 1 mm glass spheres.

The thermocouple was carefully placed in the center of the reactor bed to avoid the contact with the walls which would cause a wrong reading of the reactor temperature. For this reason, the piston displayed on the right in Figure 9 was used, with a thin tube in the middle to allow the thermocouple to slide while compacting the material around it. In order to improve compactness of the packing, a suction pump was attached at the bottom and distilled water was let flow downward. Such configuration was successful because it allowed rinses with water to push down the particles on the wall while packing, without causing the catalyst particles to float. In this way a good level of uniformity and distribution of the catalyst between the glass particles was achieved.

This process of filling was repeated until the whole 318 g of packing was efficiently placed in the reactor column. This quantity was kept the same for all the experiments with the same catalyst loading.

To block the flowing of lighter catalyst particles on the top during the experiments, a thicker layer of wet glass wool (2-3 mm) was placed and pressed over the active zone. Above the glass wool, larger size glass spheres were carefully poured over it, while pressing them down with the piston.

The final height of the bed, of ca 10 cm had the purpose of adding weight to the packing to prevent it floating away; furthermore, it also intensified the mixing after the reactive zone, upstream the sampling point. Teflon gaskets were used between the glass joints, while the silicon tubes were used to connect all parts together. In this new configuration, a manometer was also added in the bottom of the reactor to monitor possible pressure variations.

1.7 HPLC analysis of 5 hydroxy-2(5H) furanone

5 hydroxy-2(5H) furanone is one of the products formed in the reaction, with a separated peak in the HPLC chromatogram. This molecule originates from an unstable intermediate being responsible for the formation of maleic acid.

While this compound was added in the reaction mechanism based on previous publications, the retention time in HPLC and the correlation between the area and the concentration was unknown. Therefore, to obtain this information, few solutions at different concentrations were prepared. The compound, difficult to isolate, was bought from Sigma-Aldrich. Using 0.4 g of it, four solutions were prepared weighting different amounts of powder. The calculated concentration resulted to be [0.41315], [0.24789], [0.08263], [0.049578] in molar units. As done during the experiments, four labelled vials were filled with the respective solution and analysed with the HPLC refractive index detector.

The resulted area was plotted on a graph in combination with the concentrations, and a regression line was used to identify the equation of the straight line, as shown in Figure 19. This equation was used in an Excel table to automatically find the concentration of the compound given the area of the peak from the HPLC. For most of the other compounds being present in the solution, this method has been already implemented in the Laboratory. Then the results are displayed in a plot with the concentration of each compound in the y-axis and the different sampling intervals in the x-axis.

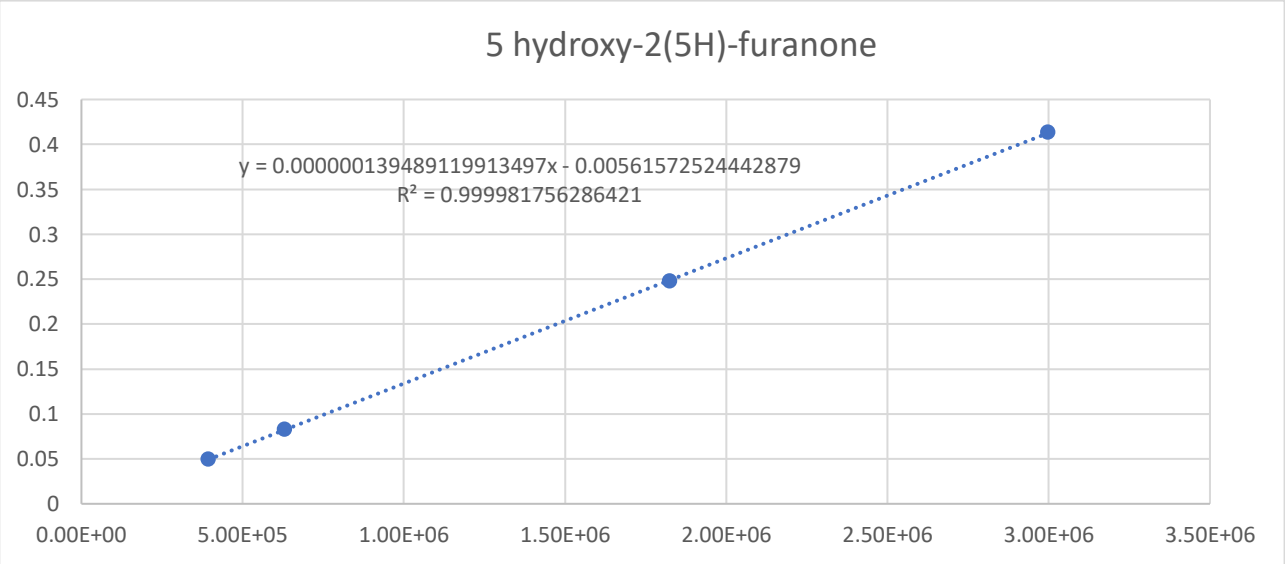

Figure 19. Regression line for the area-concentration data of 5-hydroxy-2(5H)-furanone

CHAPTER 2
EXPERIMENTAL RESULTS

2.1 Experimental conditions

Before conducting the experiments, a furfural solution with the desired concentration was prepared. Pure furfural is transparent in colour, but if it is exposed to light or air, it turns yellow to brown due to self-polymerization. For this reason, only a small amount of solution was prepared each time and filtration was necessary to remove the brown-black resin residue which might block the pores of the catalyst.

To ensure the repeatability of the experiments, a standard experiment, at 80°C, 56 ml/min and 0.5 molar solution of furfural, was repeated three times. The first experiment was performed with an old catalyst, while fresh ones were used for experiments 2 and 3. This approach served to get practice with the equipment and the analysis process. These three results showed almost similar product selectivity towards succinic and maleic acid and concentration profiles, indicating very good repeatability of the experiments, allowing further experiments at different conditions to be done.

Key experiments with variations in the operating conditions are summarized in Table 6, with highlighting the differences from the three initial standard experiments.

Table 6, List of experiments highlighting the different operating condition from the standard one.

Test nr	Furfural concentration (Molar)	HP/Fu ratio	Temperature (°C)	Flow rate (ml/min)	Percent of Catalyst to Furfural	Furfural solution volume (ml)	Duration (hours)
1	0.5	4	80	56	50	333	7
2	0.5	4	80	56	50	333	7
3	0.5	4	80	56	50	333	7
4	0.5	4	80	28	50	333	7
5	0.5	4	60	56	50	333	7
6	0.5	4	70	56	50	333	7
7	0.5	4	80	110	50	333	7
8	0.7	4	80	56	50	238	7
9	0.5	4	80	56	75	222	7
10	0.5	4	80	42	50	333	7
11	0.5	4	80	56	50	333	24
12	0.5	7	80	56	50	333	7

In all the following concentration profiles plots presented in the next pages, hydrogen peroxide is not shown, allowing to focus better on the lower concentration components which are the keys in understanding the reaction mechanism.

All the experiments were conducted while trying to maintain the temperature constant and ensure isothermal conditions for the subsequent analysis of the experimental data. Larger fluctuations were present at the beginning after the two solutions were mixed in the tank and when the flow was routed to the packed bed reactor. Smaller fluctuations and minor deviations from the fixed value were registered during the entire duration of the experiments. In the end, an average value of the registered temperature was used for modelling.

In the following pages, a summary for each experiment is shown with the operating conditions, along with conversion and selectivity as the performance indicators.

Selectivity both for succinic acid and maleic acid was calculated using the following equation:

$$S_x = \frac{Final\ concentration\ of\ x}{Initial\ concentration\ of\ furfural - final\ conentration\ of\ furfural} * 100 \qquad (3)$$

While for the conversion of furfural the following expression was used:

$$X_{Fu} = \frac{Concentration\ of\ Fu\ at\ the\ beginning - Concentration\ of\ Fu\ at\ the\ end}{Concentration\ of\ Fu\ at\ the\ beginning} * 100 \qquad (4)$$

2.2 Summary of the experiments

Below experimental conditions and the corresponding results are collected in Tables 7-18 and Figures 23-34.

The first experiment was conducted with an old catalyst (approx. 20 years), while from experiments 2 onwards, a recently purchased Amberlyst-15 was used.

Experiment 1

Table 7. Experiment 1, operating conditions and catalytic results.

Exp nr	Furfural concentration mol/L	HP/Fu ratio	Temperature °C	Flow rate ml/min	Mass ratio of wet catalyst to furfural	Furfural solution volume ml	Duration hours
1	0.5	4	80	56	0.5	333	7

Selectivity to Succinic Acid	Selectivity to Maleic Acid	Conversion of Furfural
33.4%	8.3%	100%

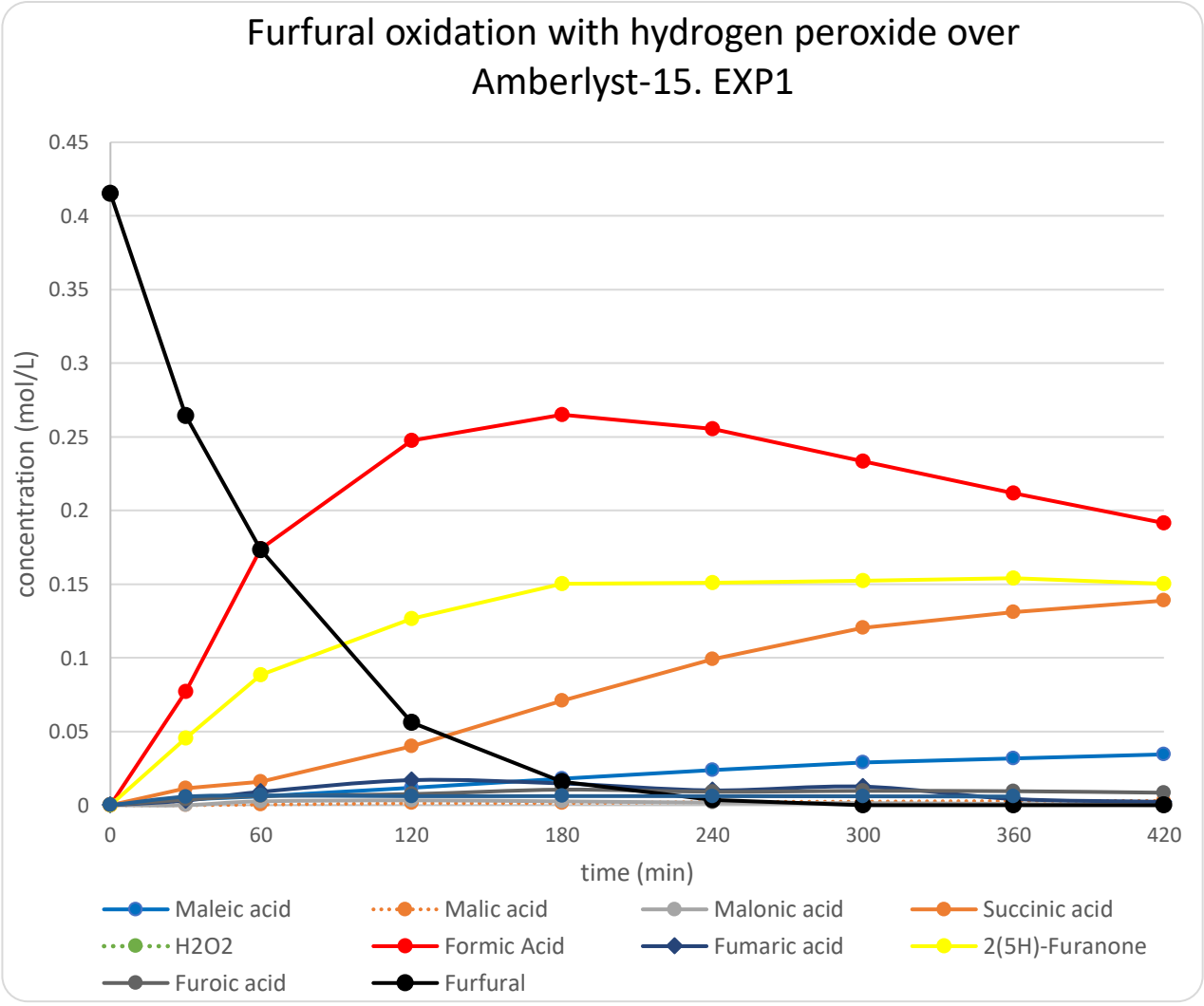

Figure 23. Experiment 1, concentration profiles.

Experiment 2 and 3

Table 8. Experiment 2 and 3, operating conditions and catalytic results

Exp nr	Furfural concentration mol/L	HP/Fu ratio	Temperature °C	Flow rate ml/min	Mass ratio of wet catalyst to furfural	Furfural solution volume ml	Duration hours
2, 3	0.5	4	80	56	0.5	333	7

Exp	Selectivity to Succinic Acid	Selectivity to Maleic Acid	Conversion of Furfural
2	36.4%	10.8%	100%
3	36.9%	9.8%	100%

In Figure 24, the data-points of experiment 2 are displayed with a circle, while for experiment 3, triangles are used. Only the main components are shown to avoid confusion with the lower concentrations.

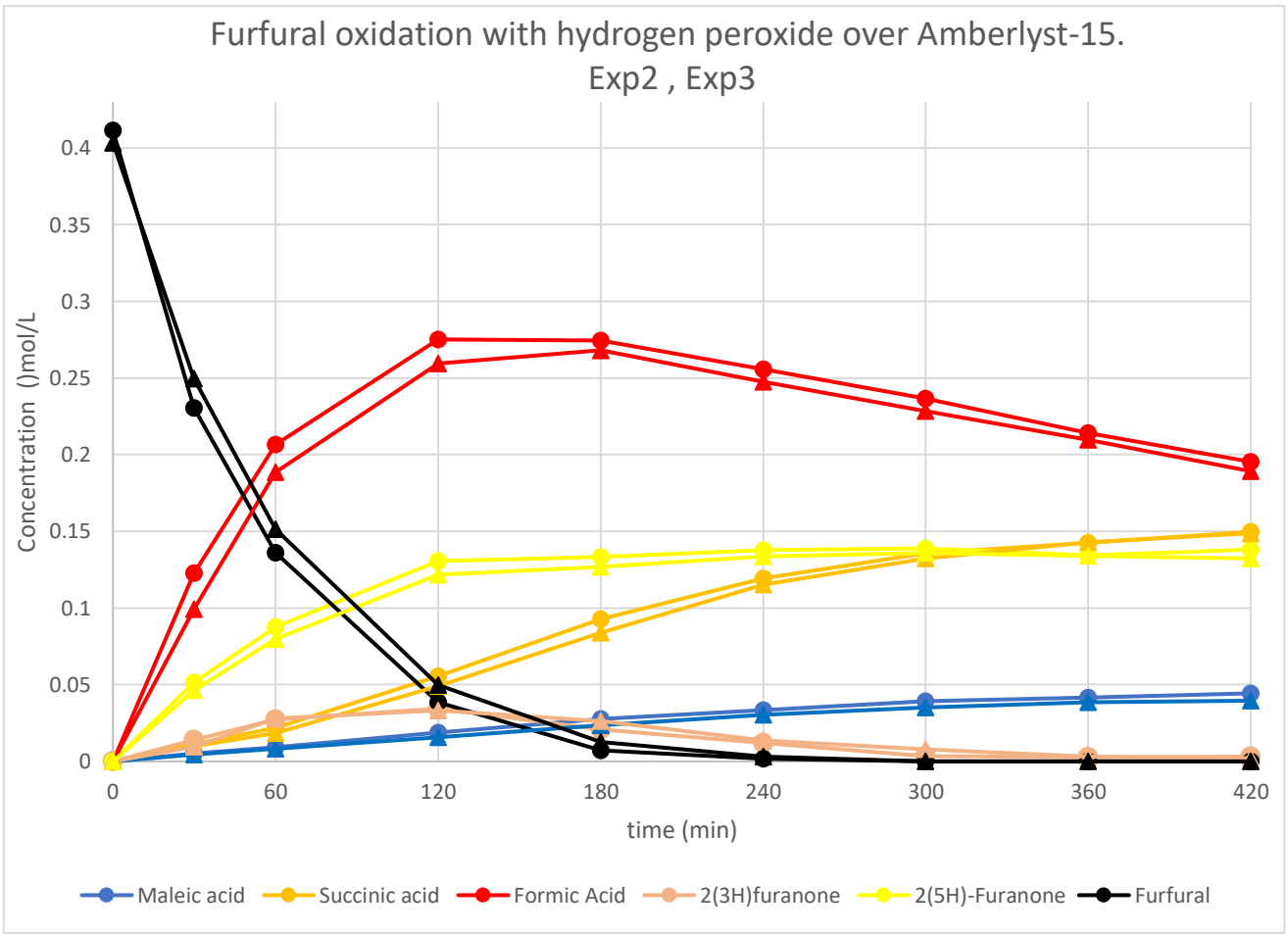

Figure 24. Experiment 2 and 3, concentration profiles.

Experiment 4

Table 10. Experiment 4, operating conditions and catalytic results.

Exp nr	Furfural concentration [Molar]	HP/Fu ratio	Temperature °C	Flow rate ml/min	Mass ratio of wet catalyst to furfural	Furfural solution volume ml	Duration hours
4	0.5	4	80	28	0.5	333	7

Selectivity to Succinic Acid	Selectivity to Maleic Acid	Conversion of Furfural
34.8%	9.4%	100%

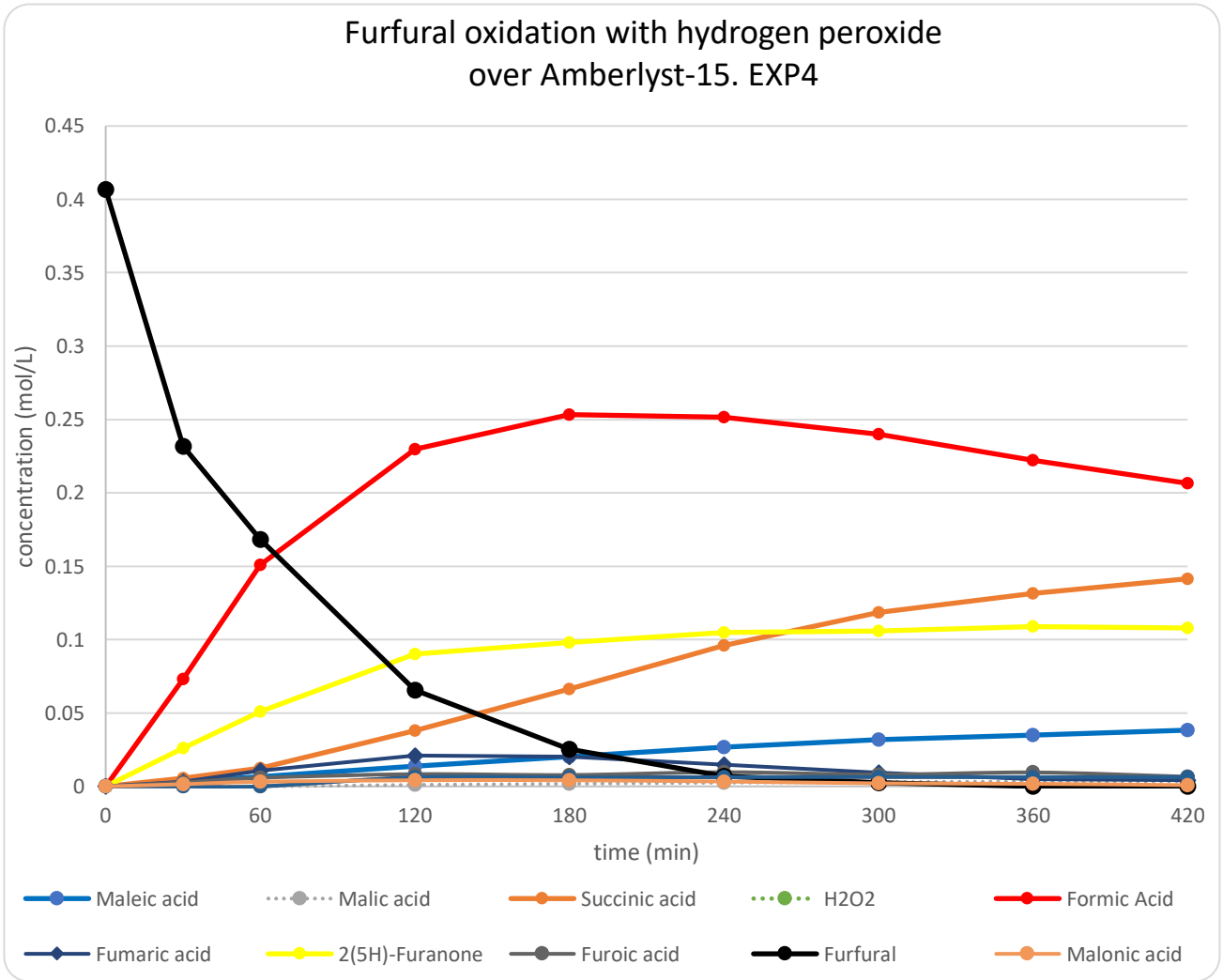

Figure 26. Experiment 4, concentration profiles.

Experiment 5

Table 11. Experiment 5, operating conditions and catalytic results.

Exp nr	Furfural concentration mol/L	HP/Fu ratio	Temperature °C	Flow rate ml/min	Mass ratio of wet catalyst to furfural	Furfural solution volume ml	Duration hours
5	0.5	4	60	56	0.5	333	7

Selectivity to Succinic Acid	Selectivity to Maleic Acid	Conversion of Furfural
15.2%	3.8%	96.8%

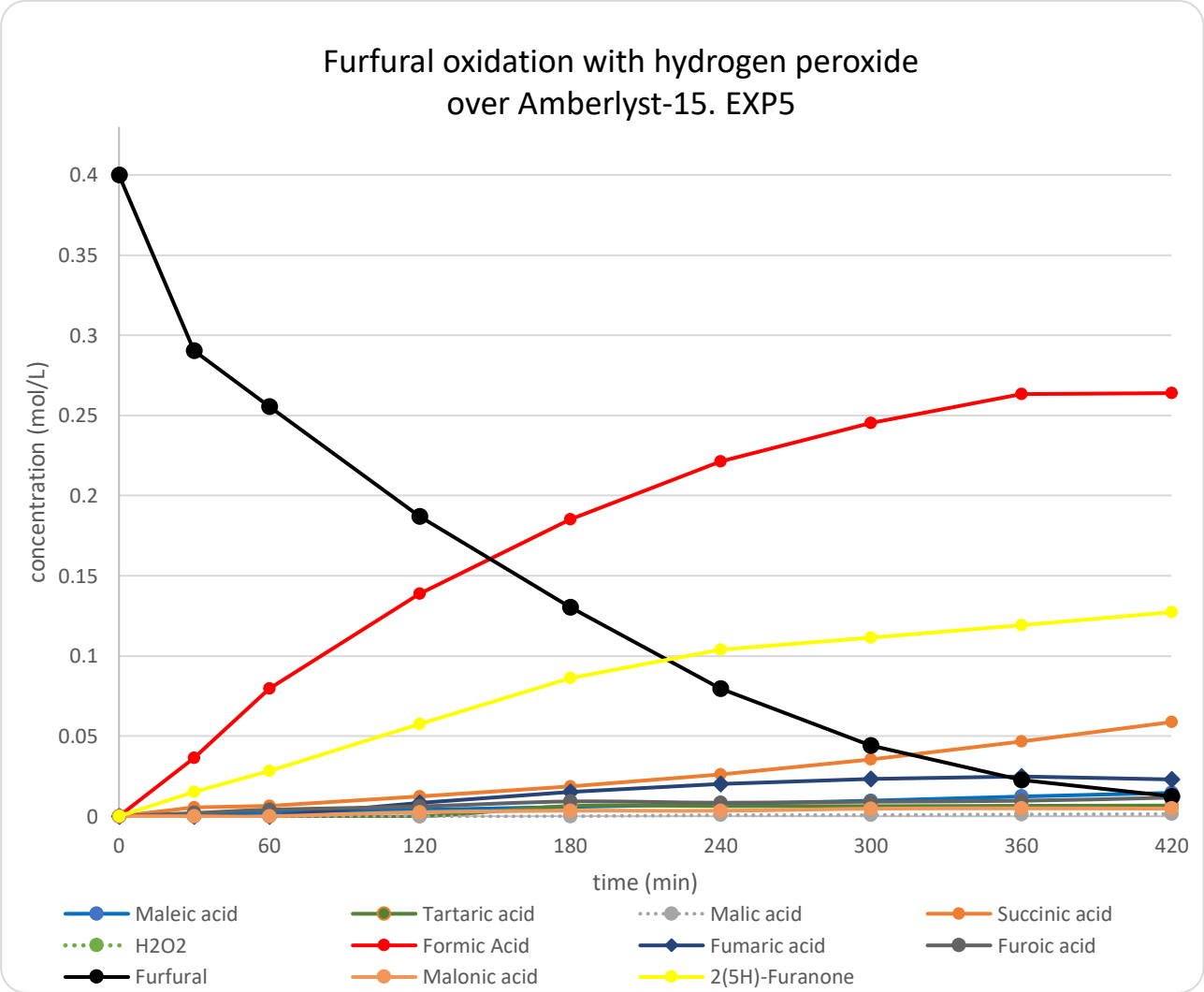

Figure 27. Experiment 5, concentration profiles.

Experiment 6

Table 12. Experiment 6, operating conditions and indicator results.

Exp nr	Furfural concentration mol/L	HP/Fu ratio	Temperature °C	Flow rate ml/min	Mass ratio of wet catalyst to furfural	Furfural solution volume ml	Duration hours
6	0.5	4	70	56	0.5	333	7

Selectivity to Succinic Acid	Selectivity to Maleic Acid	Conversion of Furfural
26.2%	6%	100%

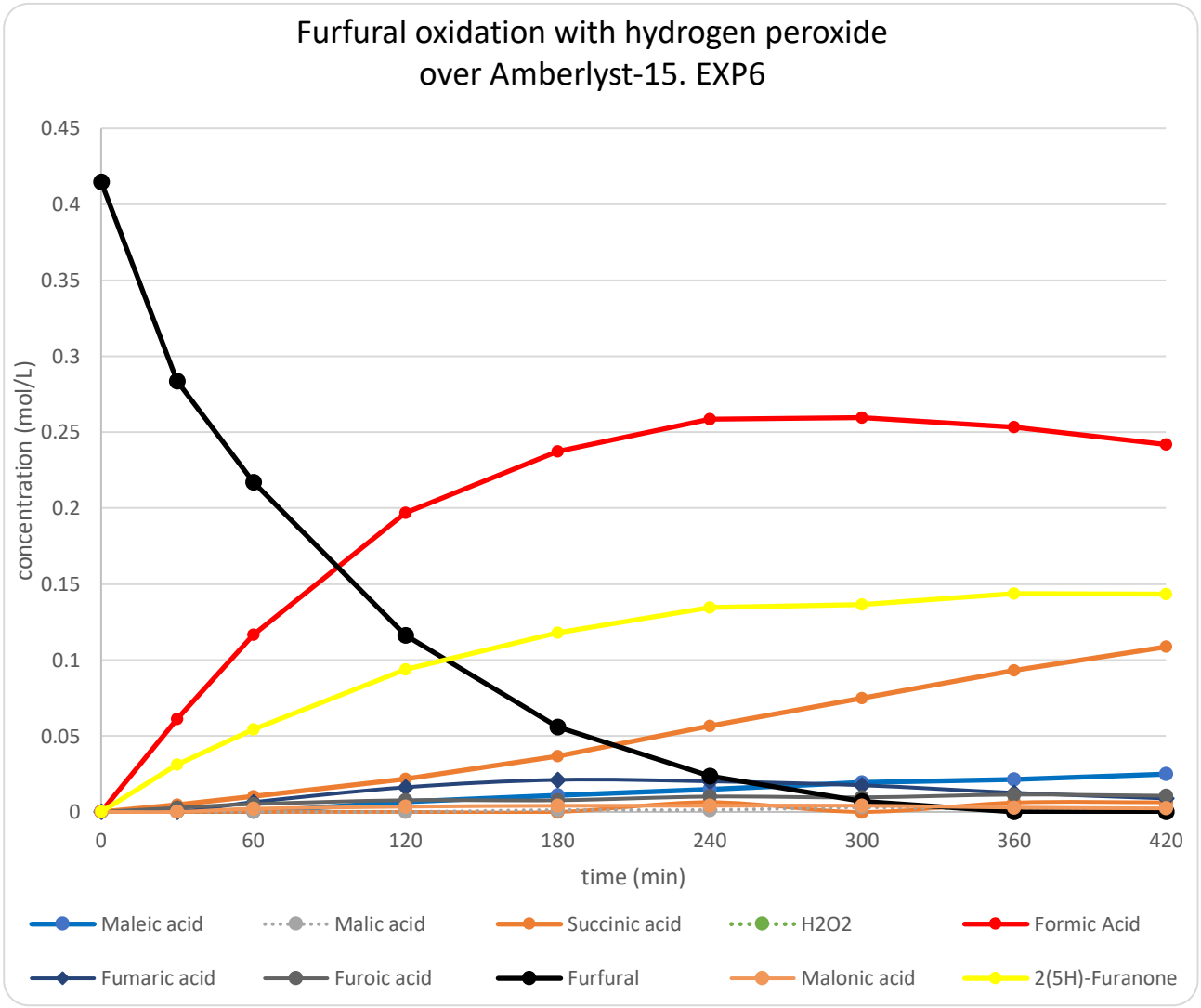

Figure 28. Experiment 6, concentration profiles.

Experiment 7

Table 13. Experiment 7, operating conditions and catalytic results.

Exp nr	Furfural concentration mol/L	HP/Fu ratio	Temperature °C	Flow rate ml/min	Mass ratio of wet catalyst to furfural	Furfural solution volume ml	Duration hours
7	0.5	4	80	110	0.5	333	7

Selectivity to Succinic Acid	Selectivity to Maleic Acid	Conversion of Furfural
32.2%	7.3%	100%

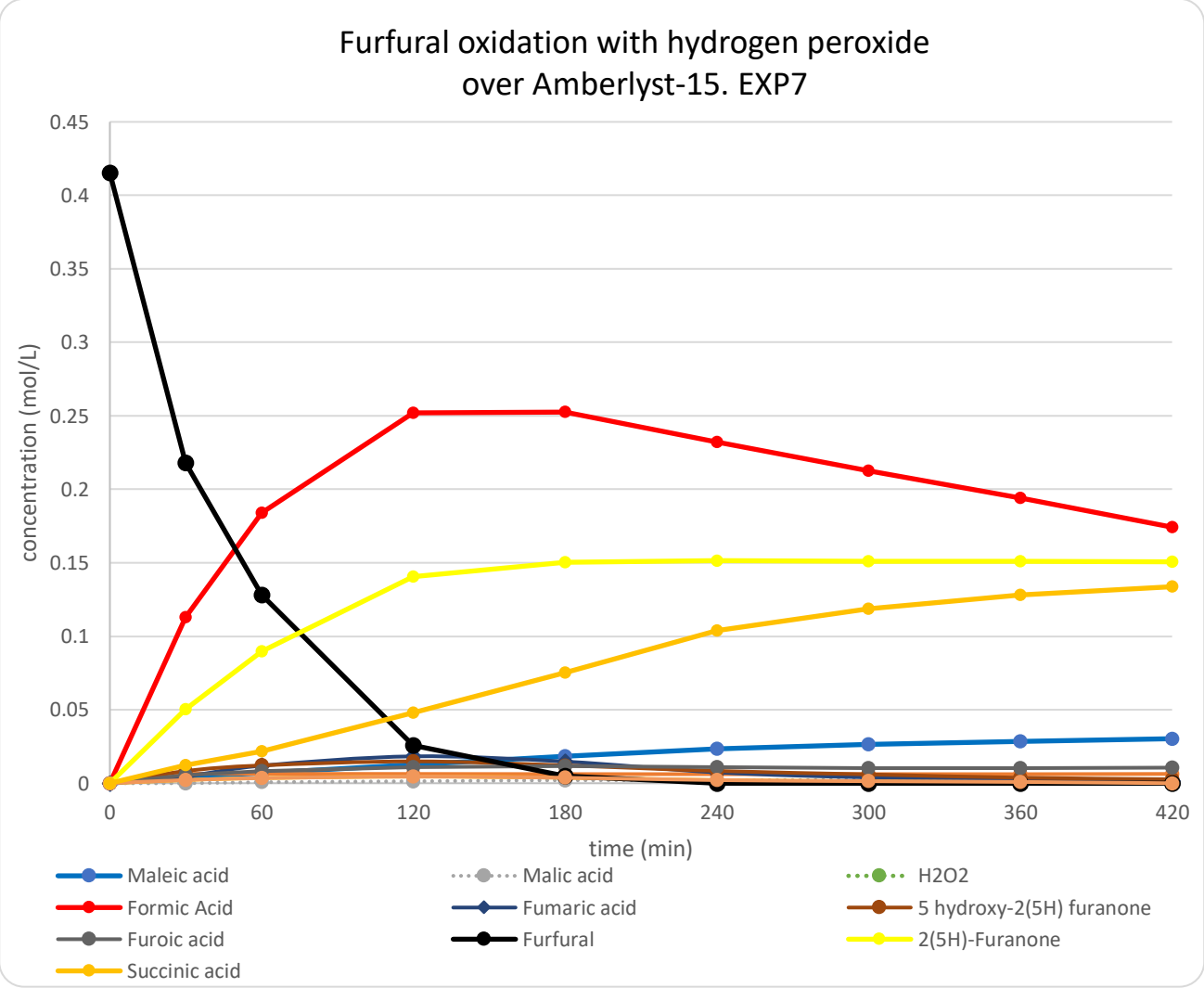

Figure 29. Experiment 7, concentration profiles.

Experiment 8

Table 14. Experiment 8, operating conditions and catalytic results.

Exp nr	Furfural concentration mol/L	HP/Fu ratio	Temperature °C	Flow rate ml/min	Mass ratio of wet catalyst to furfural	Furfural solution volume ml	Duration hours
8	0.7	4	80	56	0.5	333	7

Selectivity to Succinic Acid	Selectivity to Maleic Acid	Conversion of Furfural
34.1%	10.2%	100%

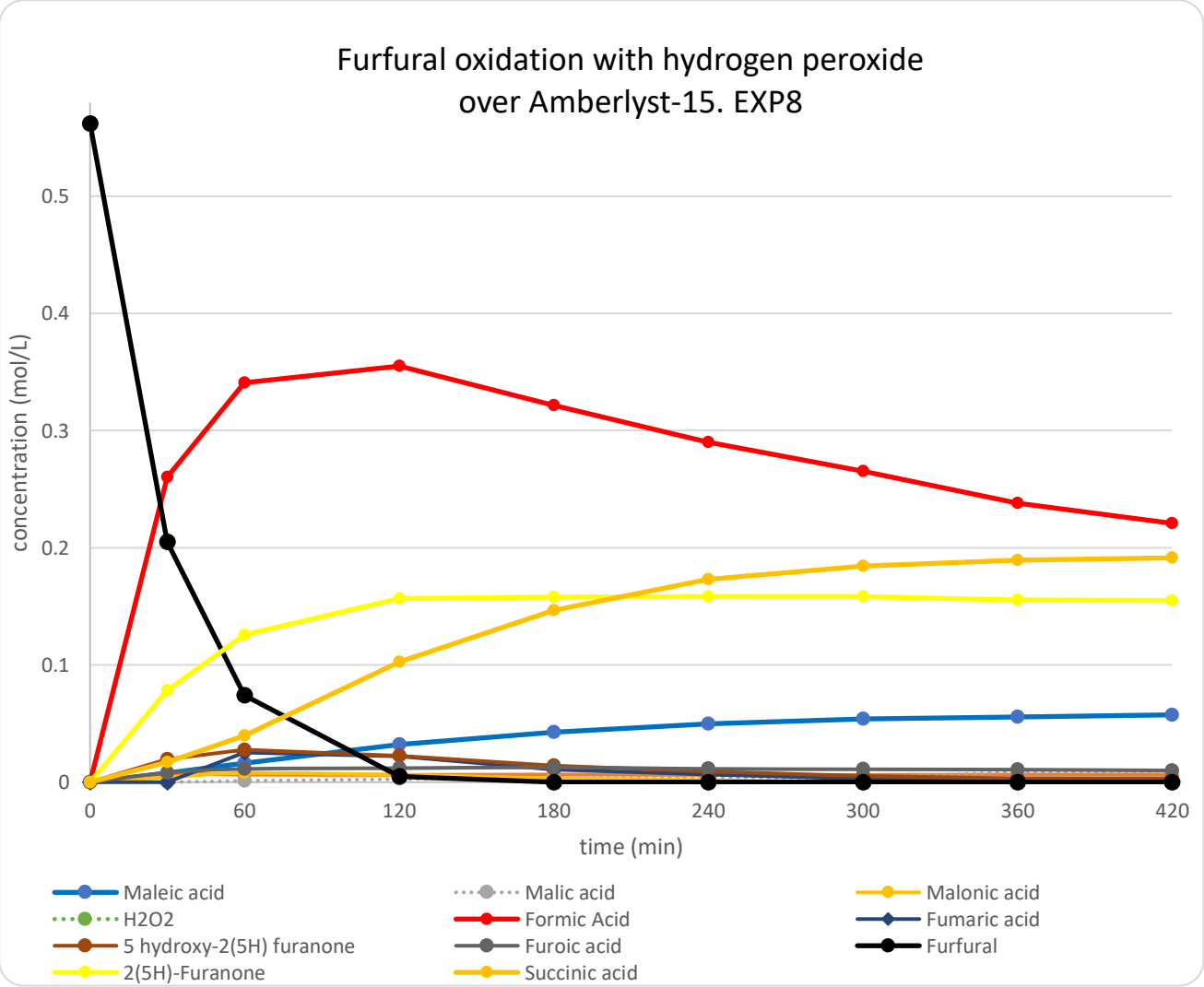

Figure 30. Experiment 8, concentration profiles.

Experiment 9

Table 15. Experiment 9, operating conditions and catalytic results.

Exp nr	Furfural concentration mol/L	HP/Fu ratio	Temperature °C	Flow rate ml/min	Mass ratio of wet catalyst to furfural	Furfural solution volume ml	Duration hours
9	0.5	4	80	56	0.75	333	7

Selectivity to Succinic Acid	Selectivity to Maleic Acid	Conversion of Furfural
29.1%	5.9%	100%

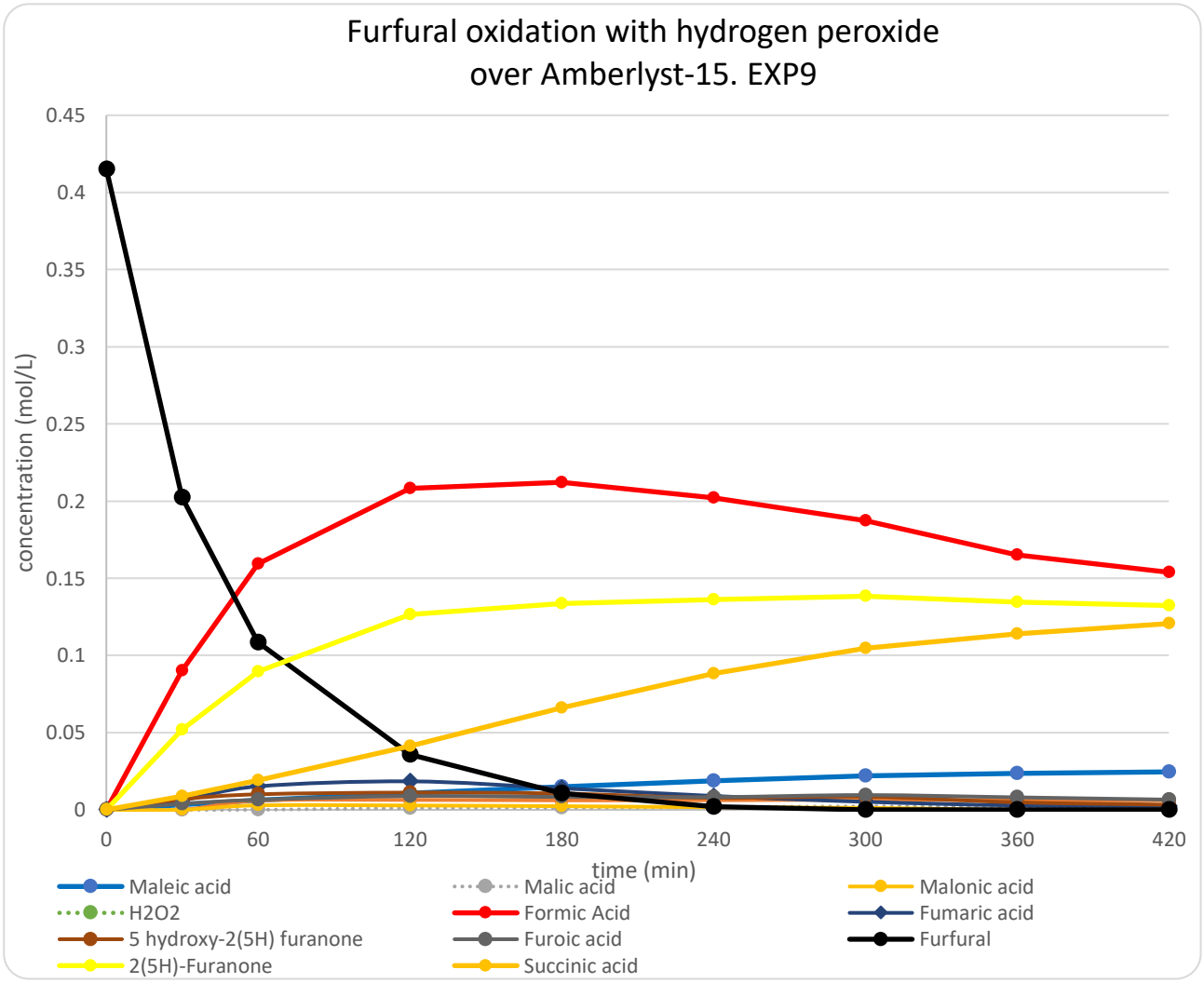

Figure 31. Experiment 9, concentration profiles.

Experiment 10

Table 16. Experiment 10, operating conditions and catalytic results.

Exp nr	Furfural concentration mol/L	HP/Fu ratio	Temperature °C	Flow rate ml/min	Mass ratio of wet catalyst to furfural	Furfural solution volume ml	Duration hours
10	0.5	4	80	42	0.5	333	7

Selectivity to Succinic Acid	Selectivity to Maleic Acid	Conversion of Furfural
33.3%	8.1%	100%

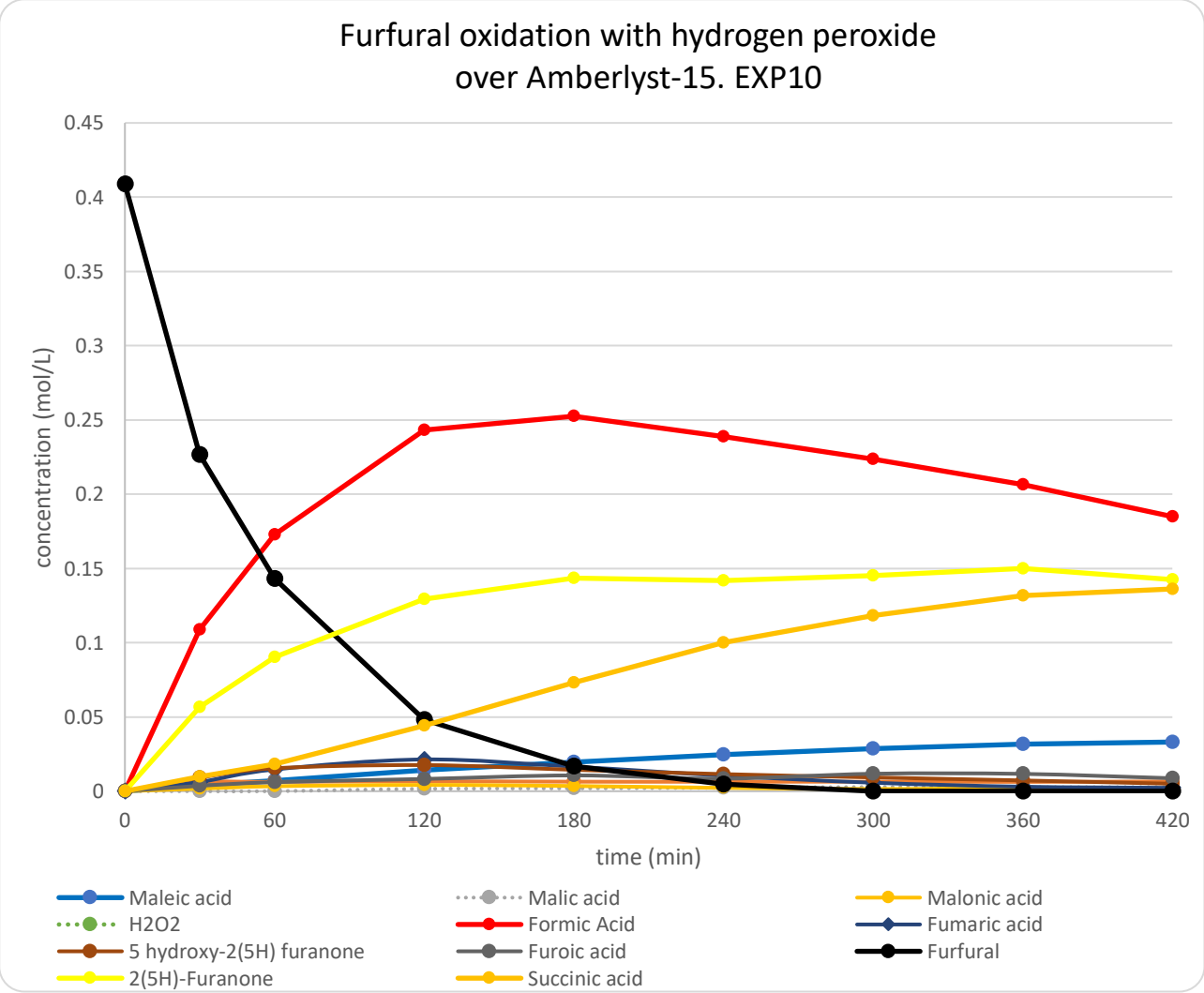

Figure 32. Experiment 10 concentration profiles.

Experiment 11

Table 17. Experiment 11, operating conditions and indicator results.

Exp nr	Furfural concentration mol/L	HP/Fu ratio	Temperature °C	Flow rate ml/min	Mass ratio of wet catalyst to furfural	Furfural solution volume ml	Duration hours
11	0.5	4	80	56	0.5	333	24

Selectivity to Succinic Acid	Selectivity to Maleic Acid	Conversion of Furfural
42.0%	8.2%	100%

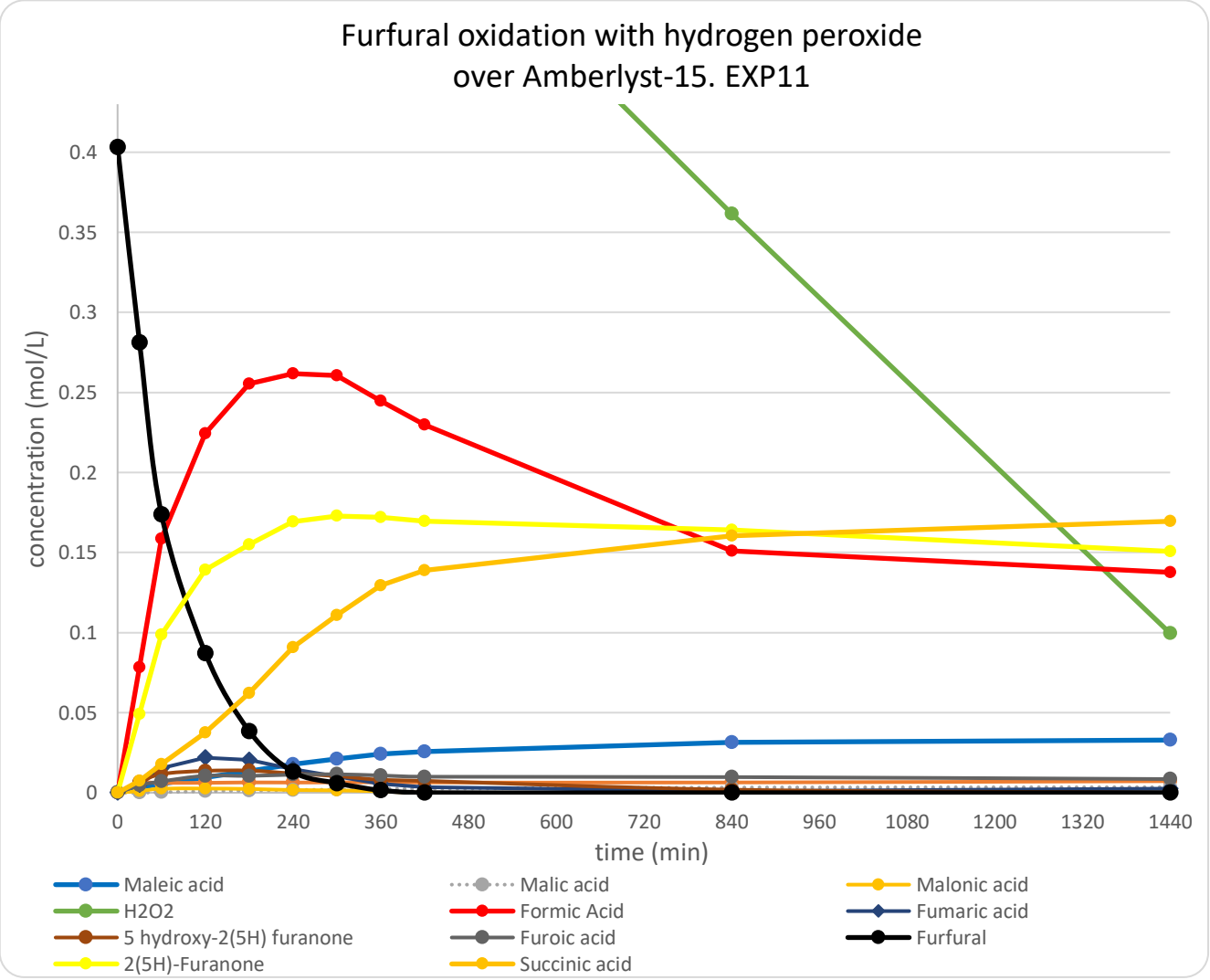

Figure 33. Experiment 11, concentration profiles.

Experiment 12

Table 18. Experiment 12, operating conditions and indicator results.

Test nr	Furfural concentration [Molar]	HP/Fu ratio	Temperature °C	Flow rate ml/min	Mass ratio of wet catalyst to furfural	Furfural solution volume ml	Duration hours
12	0.5	7	80	56	0.5	333	7

Selectivity to Succinic Acid	Selectivity to Maleic Acid	Conversion of Furfural
35.90%	11.0%	100%

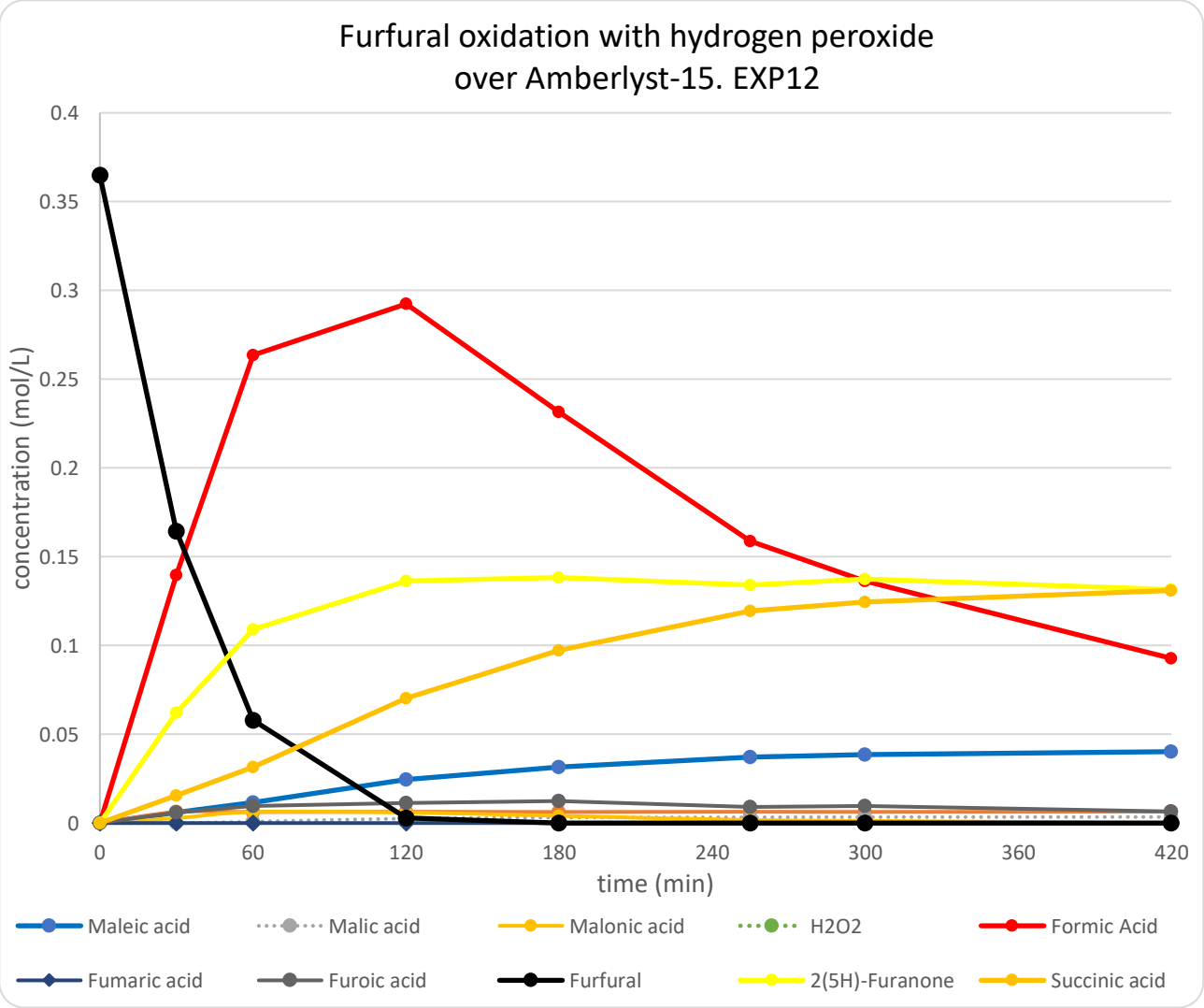

Figure 34. Experiment 12, concentration profiles.

Experiment in the absence of catalyst

A blank experiment conducted in a batch mode in the absence of catalyst was done to understand if the molecules of interest are produced non-catalytically. The test of 7 h duration was conducted at 80°C with furfural concentration of 0.5 mol/L, a ratio HP/Fu of 4 and 8 g of catalyst (50% of furfural mass).

The plot of the concentrations of the main components is shown in Figure 35; hydrogen peroxide is not shown to focus on the profiles of the other components present in small concentrations.

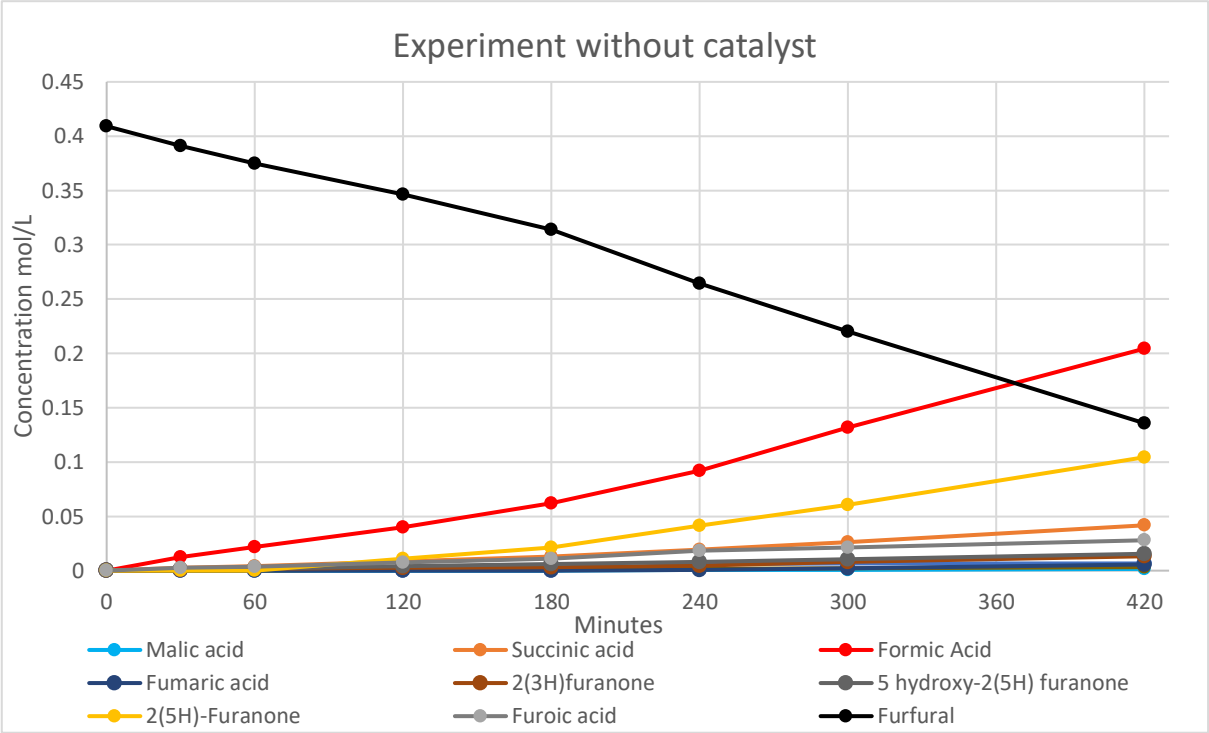

Figure 35. Blank experiment without a catalyst.

In this case, conversion of furfural was 67% after seven hours, while with the catalyst in the standard experiment the conversion reached 100% after ca four hours. Furthermore, selectivity to succinic acid in the blank experiment was 15% while in the best conditions with Amberlyst-15 a selectivity of ca 36% was achieved.

2.3 Experiments with the intermediates

To improve the understanding and to get a deeper insight of the reaction mechanism, experiments with all the stable intermediates were carried out. This allows to more precisely identify the routes through which the components at the end are formed. Mechanistic understanding is also useful for the kinetic modelling, namely for fitting the concentration profiles.

All the intermediates were delivered by trusted chemical companies in small quantities, usually around 1 g. This had the purpose of determining the retention time in HPLC and making the calibration curves.

The first experiment was conducted using a solution of the 5-hydroxy-2(5H)-furanone with hydrogen peroxide and the catalyst in a well stirred small batch reactor, for six hours at 80°C (Figure 36).

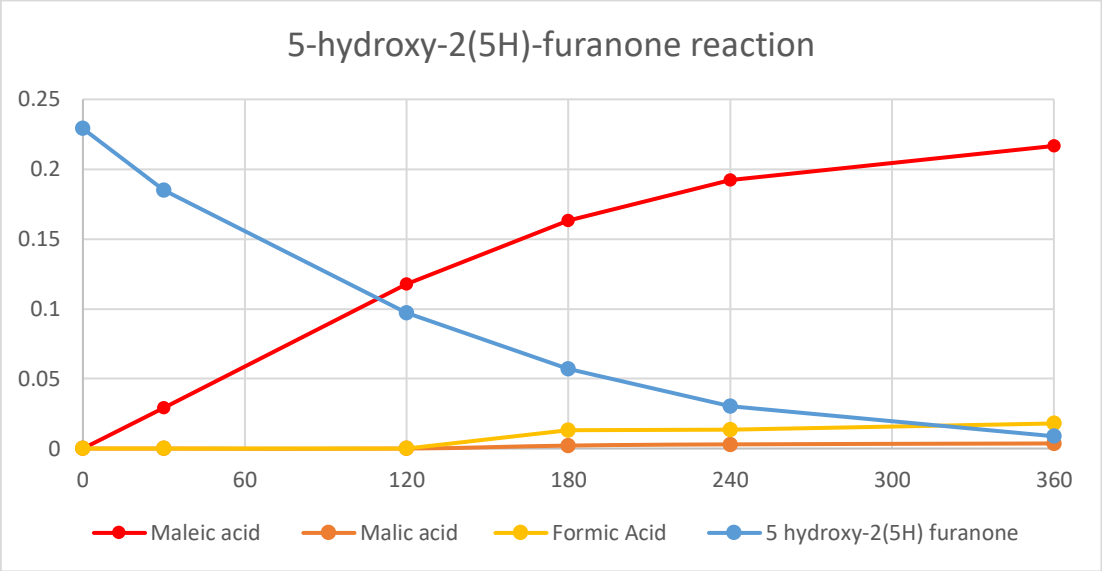

Figure 36. 5-hydroxy-2(5H)-furanone experiment in a batch reactor, at 80°C, 700 rpm, 6 h.

From the concentration profiles displayed in Figure 36 it is visible that the main product of this reaction is maleic acid, with a low concentration of formic and malic acids. These two last components are products of maleic acid reaction with hydrogen peroxide.

Then furoic acid was tested under identical experiment conditions, resulting in a flat profile for furoic acid and a minor decomposition of hydrogen peroxide due to the elevated temperature (Figure 37).

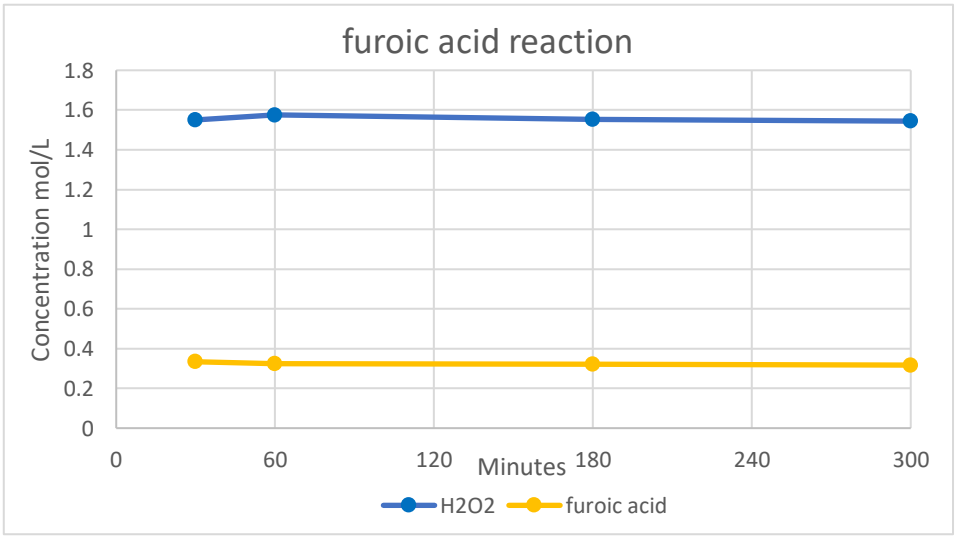

Figure 37. Furoic acid experiment in a batch reactor, at 80°C, 700 rpm, 6 h.

It was therefore concluded that furoic acid is non reacting under the experimental conditions.

For 2(5H)-furanone, the result was almost the same as for furoic acid, showing only formation of trace amounts of succinic acid. Such low concentration of succinic acid from this reaction demonstrates that succinic acid is not formed from 2(5H) furanone.

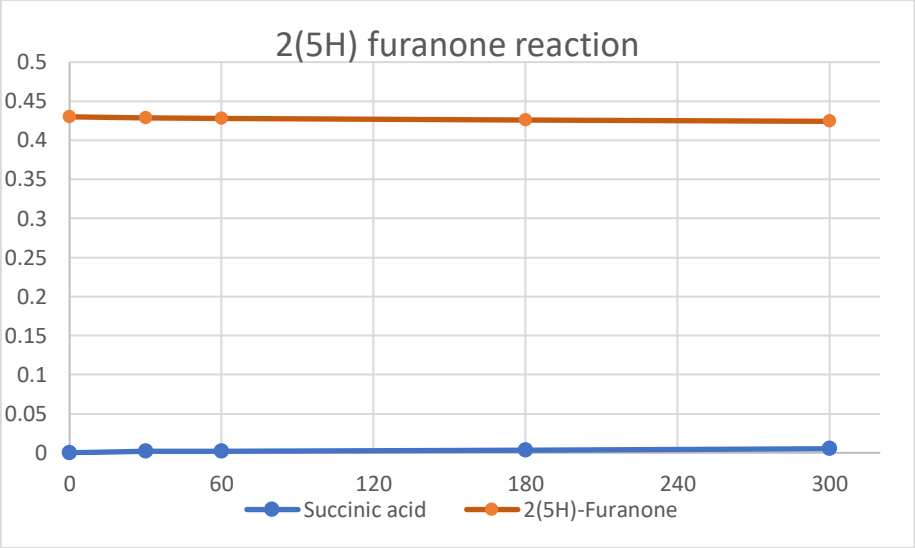

Figure 38. 2(5H) furanone experiment in a batch reactor, at 80°C, 700 rpm, 6 h.

In conclusion, 2(5H)-furanone represents a dead end in the reaction towards the desired products.

Maleic acid was ultimately tested to prove that malic, tartaric and fumaric acids were formed during the reaction with hydrogen peroxide in the presence of the catalyst.

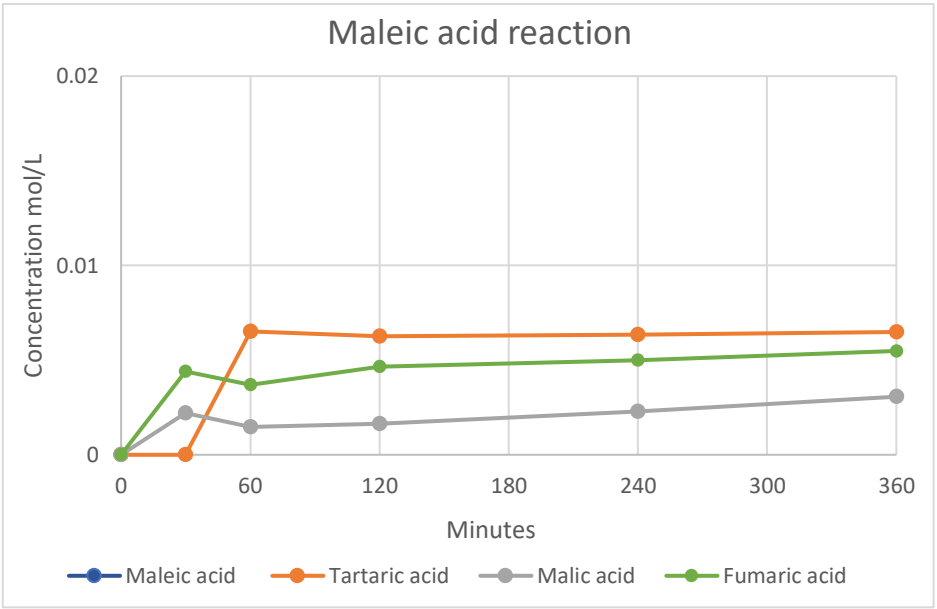

Figure 39. Maleic acid experiment in a batch reactor, at 80°C, 700 rpm, 6 h.

2.4 A newly identified intermediate and the modified reaction mechanism

At this point all the stable intermediates present in the original reaction mechanism have been tested and none of them gave a substantial yield of succinic acid. This implied that there is another route for the production of succinic acid.

Analyses of HPLC chromatograms demonstrates there were few minor unidentified products that were not considered. By plotting these areas as function of the reaction time, it was discovered that two of them where side products, as their concentrations slowly increased with time, while another one was first generated and then consumed. This variation in the concentrations indicated that it was an intermediate, as visible with a green curve in Figure 40.

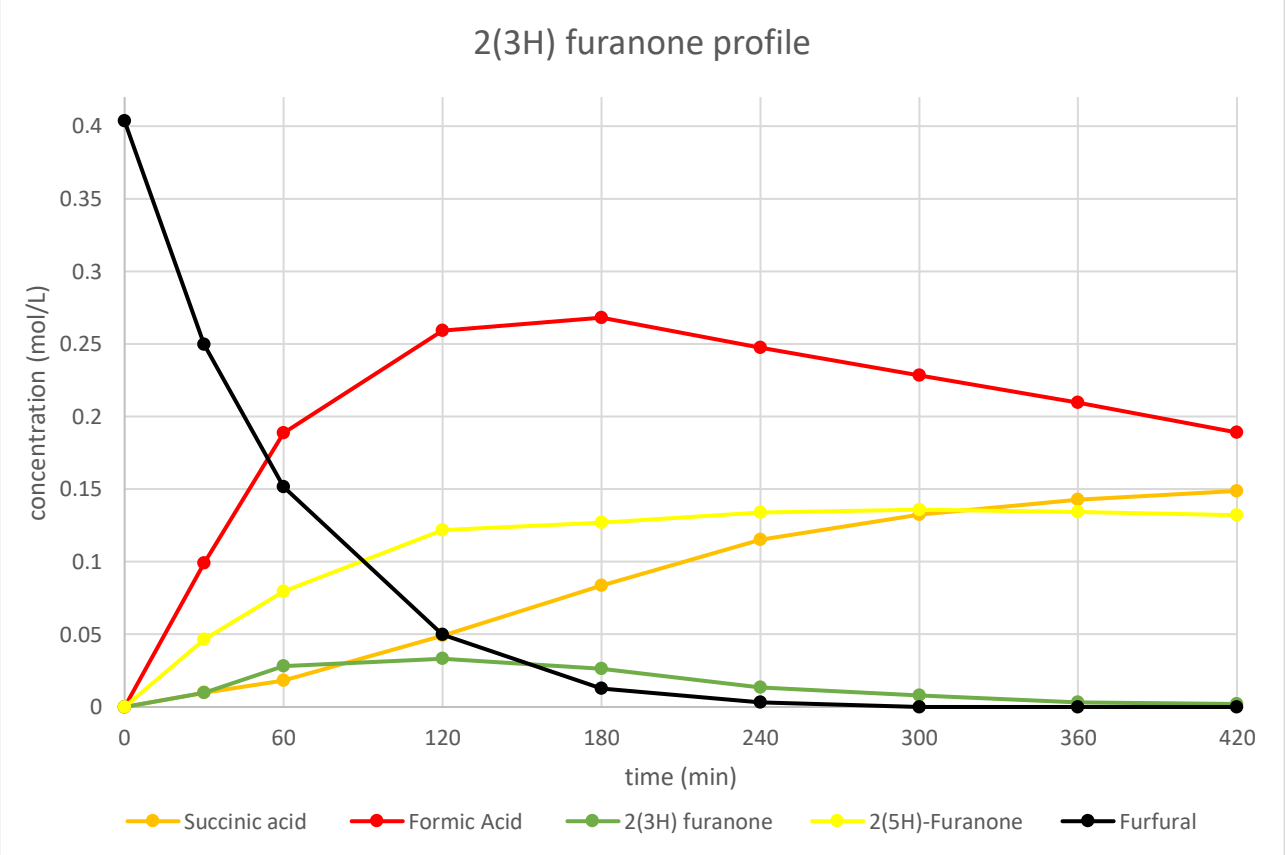

Figure 40, Concentration profiles of the main components of furfural oxidation with hydrogen peroxide; a reference experiment conducted at 80°C, 56 ml/min, 0.5 mol/L furfural concentration, 16 g of wet catalyst.

In the literature, some articles [29-30-31] included 2(3H)-furanone in oxidation reactions of furfural to succinic acid. Because 2(3H)-furanone is an isomer of 2(5H)-furanone (Figure 41), which properties were already known, it was decided to firstly use its area-concentration correlation and extend it to the missing intermediate.

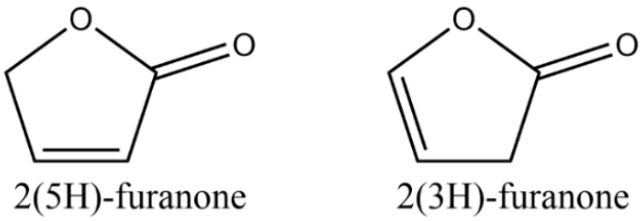

Figure 41. The two isomers.

Unfortunately, because of its instability, it was not possible to purchase a commercial sample of 2(3H)-furanone and test it in a small batch. The separation process of this compound from the other reaction products and its isomer would have been too complicated and unfeasible within the framework of this thesis work.

Several reaction mechanisms have been used and modified to reach a satisfying fitting of the experimental data. Initially, the previous mechanism displayed in Figure 11 was improved considering the results of the experiments with the intermediates. For example, the reaction from 5-hydroxy-2(5H)-furanone to succinic acid was omitted, along with the reaction of 2(5H)-furanone to maleic acid was removed while a new route with 2(3H)-furanone to succinic acid was added. Later, new reaction paths and unstable intermediates were added, according to the atomic rearrangements between the molecules, to explain the shapes of the concentration profiles.

The process of fitting with the parameter estimation and the results of the experiments with the intermediates resulted in a new reaction mechanism which is presented in Figure 42.

In total, 25 reactions are included in the mechanism which describe the stoichiometry in the kinetics of the product formation. As it will be presented in the Kinetic modelling chapter, some reactions are really slow, while others are almost instantaneous.

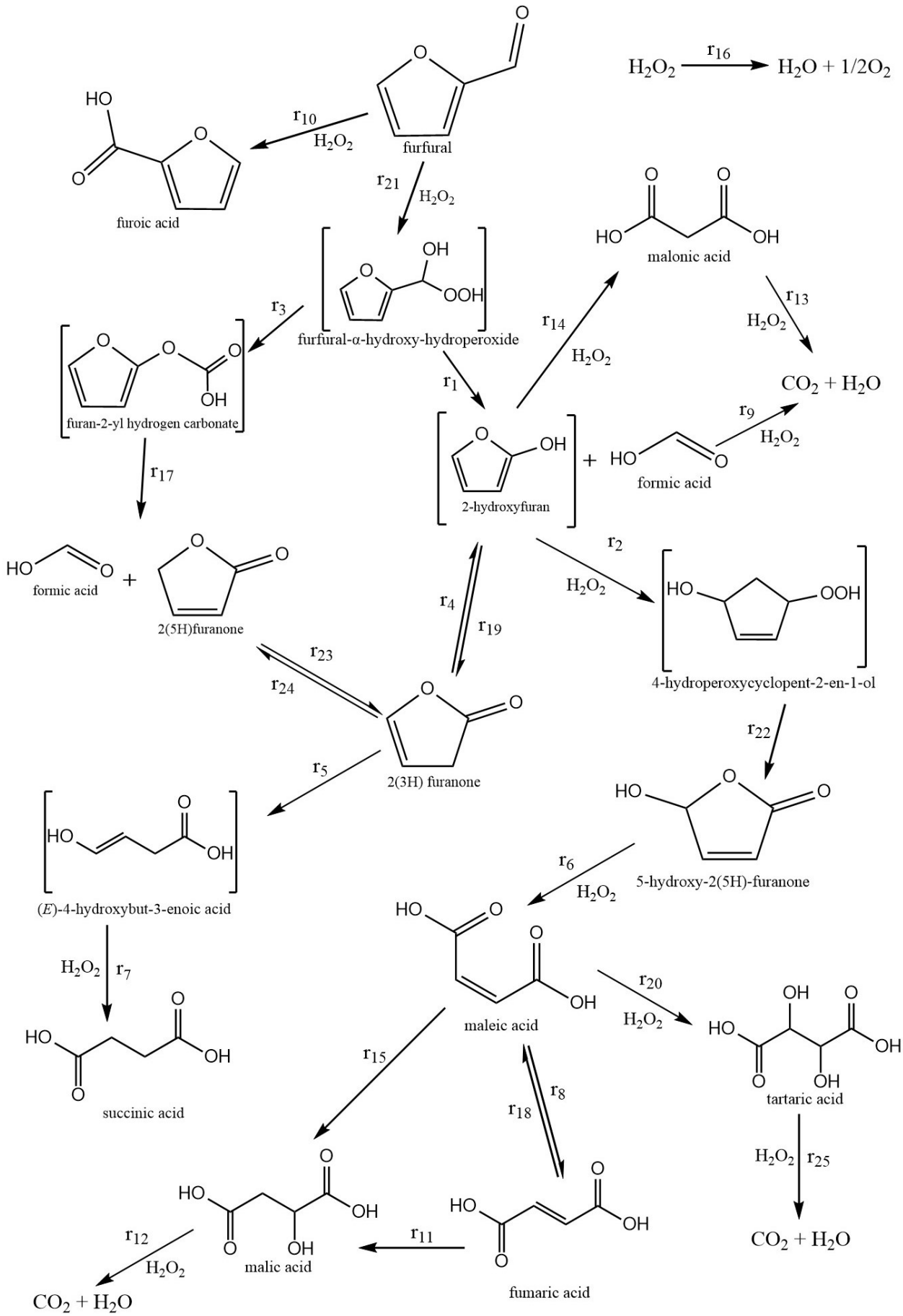

Fig 42. Improved reaction mechanism

2.5 Comparison of the experiments

In this section, the experimental results are compared with each other to understand the best conditions to conduct this process.

In Figure 43, the only operating condition that differs between the experiments is the reactor temperature, while the other experimental parameters are maintained constant. The molar ratio of hydrogen peroxide-to-furfural was 4, and the initial concentration of furfural was about 0.5 mol/L, furthermore, the catalyst amount was kept the same with 8 g and the flowrate was 56 ml/min.

Two experiments at the same temperature in red and blue colours are demonstrated to visualize the repeatability of the experiments. The slight difference is probably due to the difficulty of keeping the temperature at 80°C for the entire reaction time; in fact, often fluctuations between 79°C and 81°C were observed. Nevertheless, it is clear that the reaction temperature highly affects selectivity to succinic acid formation.

In the end, not only selectivity is impaired when lowering the reactor temperature, but also the conversion of furfural is retarded because of slower reaction kinetics, which leads to a lower concentration of succinic acid at the end of seven hours experiment.

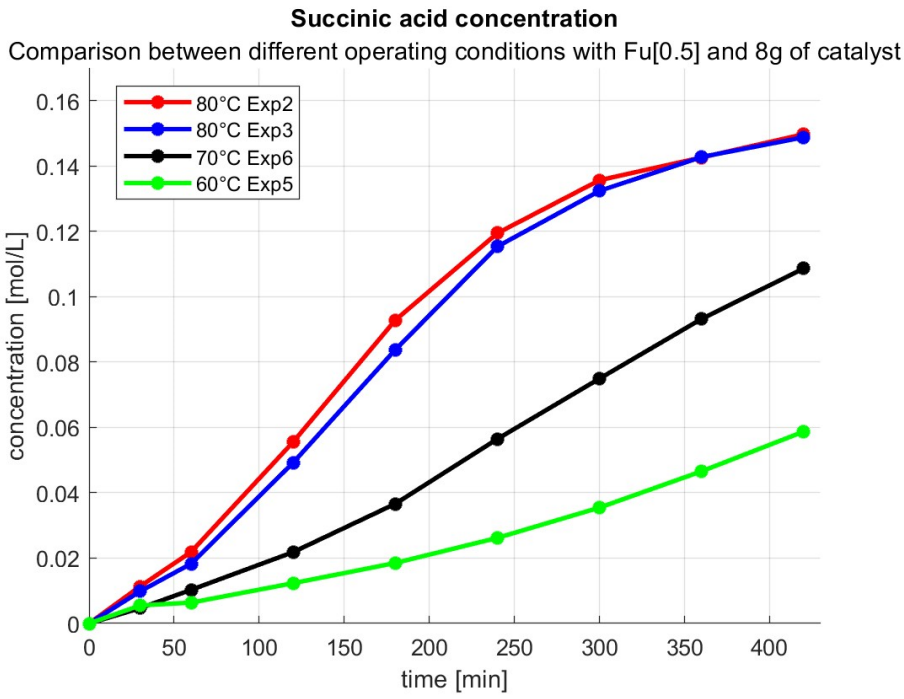

Figure 43. Succinic acid concentration as a function of the reaction time.

Variation in concentrations at different flow rates are shown in Figure 44.

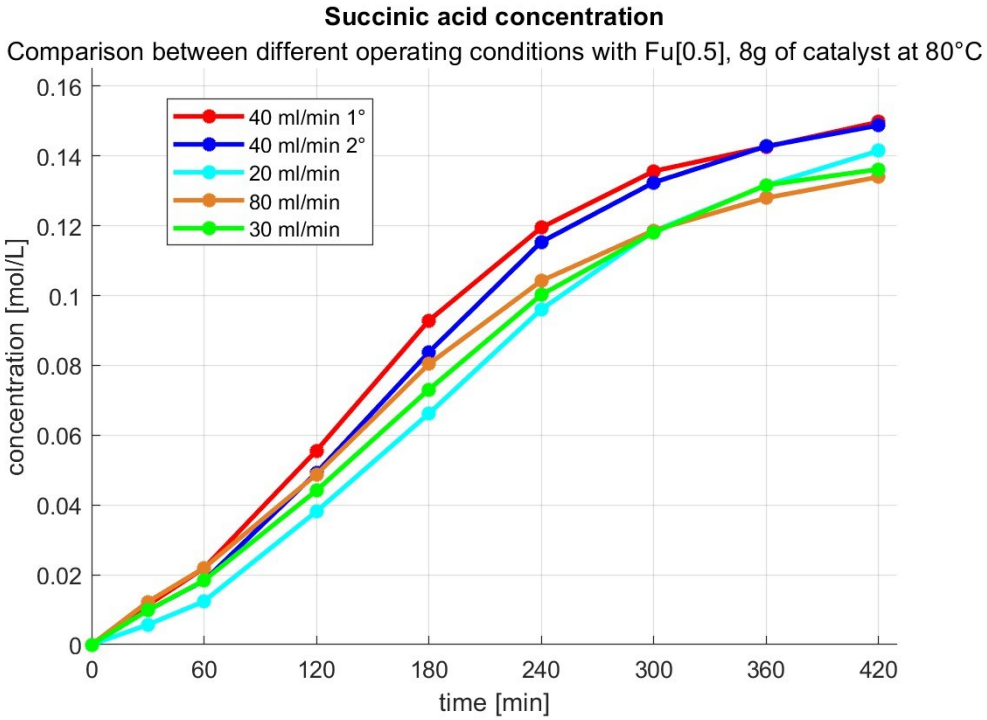

Figure 44. Succinic concentration profiles at different flow rates.

Such variations did not have a very strong impact on the concentration and selectivity of succinic acid, with 56 ml/min flow rate resulting in the best performance.

Figure 45 shows dependance of succinic acid yields at different initial concentration of furfural and hydrogen peroxide.

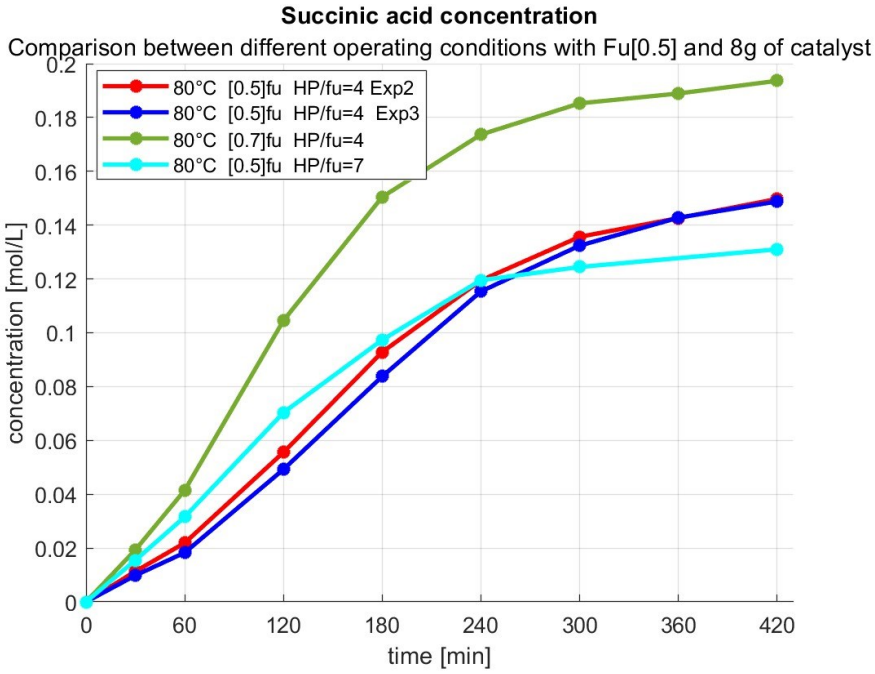

Figure 45. Succinic acid concentration profiles varying other parameters.

Besides the higher final concentration of succinic acid from the experiment with 0.7M of furfural which is proportional to the initial amount of furfural, the selectivity profiles are rather similar. Just a small decrease of the selectivity was noticed as the furfural initial concentration was higher. What changes are the profiles between one and three hours, which resulted in a faster production as furfural was more concentrated or there is more hydrogen peroxide in the solution; anyway, they eventually settle as the standard experiment after seven hours.

A higher furfural concentration is thus giving a higher final concentration of succinic acid at the same reaction time and operating conditions. Because furfural solubility in water at 20°C is low, close to 0.75 mol/L, it would be useful to mix furfural and water at a higher temperature, before sending the mixture to the reactor.

Furthermore, higher temperatures improve the reaction kinetics, in this case preserving high selectivity to succinic acid.

If the only product of interest is succinic acid, then maleic acid can be later hydrogenated to directly produce it [32].

2.6 Different catalysts screened in selective oxidation of furfural

While carrying out the main study in the PBR with Amberlyst-15, complementary experiments were done with other catalysts in oxidation of furfural to succinic acid. The experiments were conducted in small, stirred vials of 10 ml, immersed in an oil bath to keep the temperature at 80°C for six hours.

Several catalysts were tested because they had performed well in other oxidation reactions and having similar acidity as Amberlyst-15. Other catalysts, promising in terms of selectivity, not readily available in the laboratory, will be tested in the future as a part of a similar study.

The first catalyst was Ni/αAl_2O_3, because a similar catalyst with nickel deposited on a ceramic (LDH) [24] was applied in the furfural oxidation. A batch experiment with the catalyst powder was done, showing low selectivity towards succinic acid, generating substantial amounts of formic acid. It was hence discarded from the future tests.

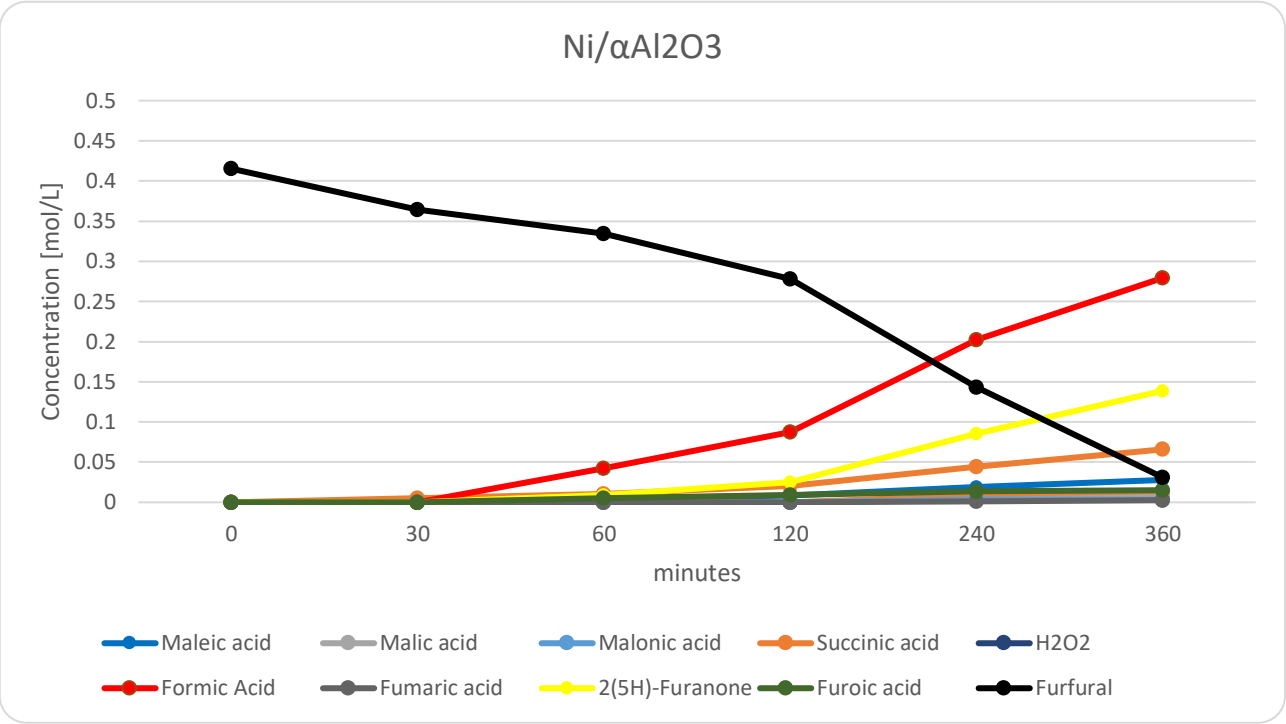

Figure 12. Concentration profiles in furfural oxidation with H_2O_2 over $Ni/\alpha Al_2O_3$. (Batch, 80°C, 6 h, 700 rpm)

TS-1 titanium silicalite zeolite was used because of a good performance in selective oxidation of organic compounds. In a batch experiment, high selectivity towards maleic acid was obtained without the formation of succinic acid (Figure 13). At the same time, substantial amounts of formic were formed.

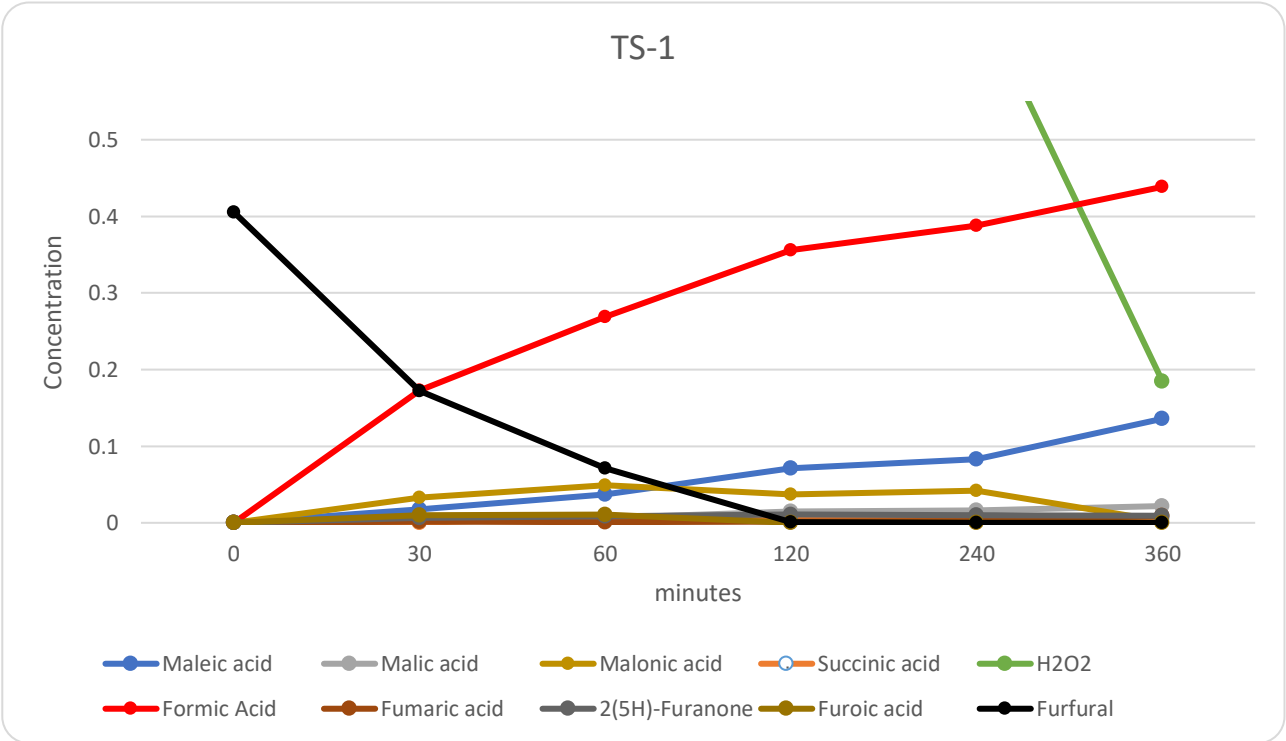

Figure 13. Concentration profiles in furfural oxidation with H_2O_2 over TS-1. (Batch, 80°C, 6 h, 700 rpm)

In another article [25], a tin catalyst with very good performances in this kind of oxidation was reported, therefore it was decided to test tin on different supports. Results for Sn MgO from batch reactor tests are presented in Figure 14. Even worse selectivity towards the two products of interest (succinic and maleic acids) was noticed, while decomposition of furfural to formic acid was profound.

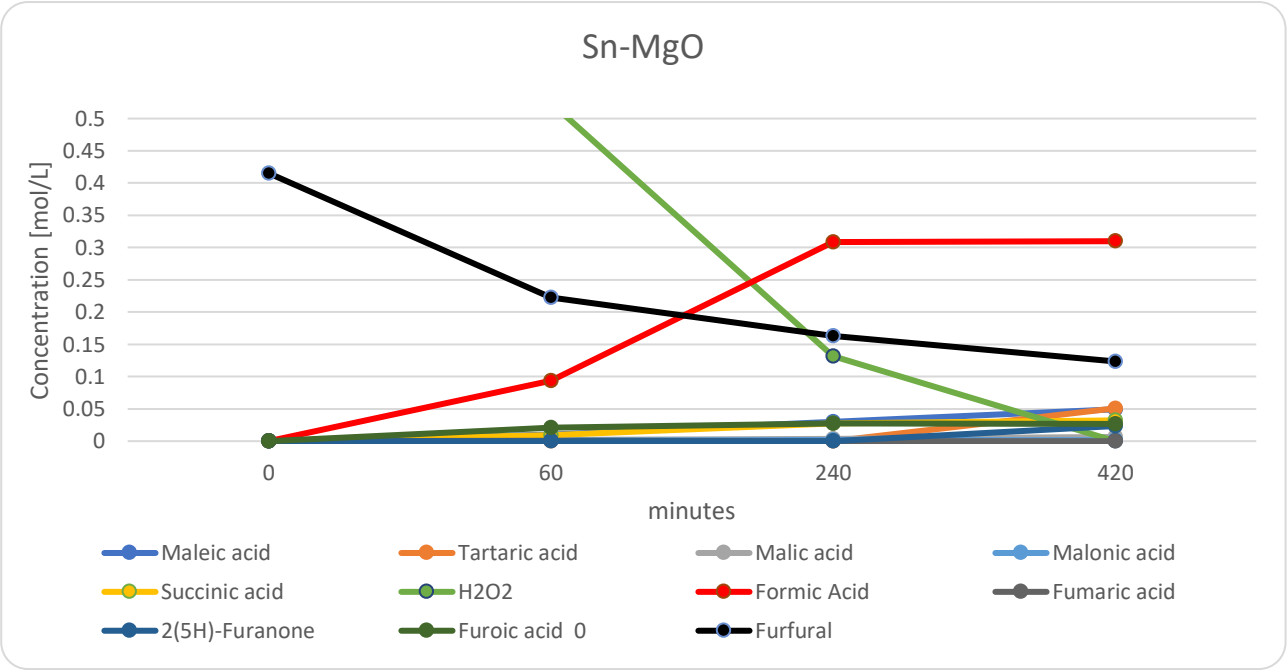

Figure 14. Concentration profiles in furfural oxidation with H_2O_2 over Sn-MgO. (Batch, 80°C, 6 h, 700 rpm)

Tin deposited on alumina (Sn-Al_2O_3) was prepared specifically for furfural oxidation.

First, 1.25 g of tin chloride dihydrate was dissolved in 200 ml of distilled water, to obtain 0.5 g of tin deposited on 10 g of alumina. Spherical particles of Al_2O_3 were crushed in a mortar to obtain a fine powder. In case of packed bed reactor, the spherical alumina particles can be used directly as a support for the tin.

After dissolution of the salt, the powder was added to the solution in a glass vessel, which was connected to a rotary evaporator for 24 hours at 60°C allowing the solution to be adsorbed by the support. After 24 hours the vacuum pump was turned on to dry completely the catalyst as visualized in Figure 15.

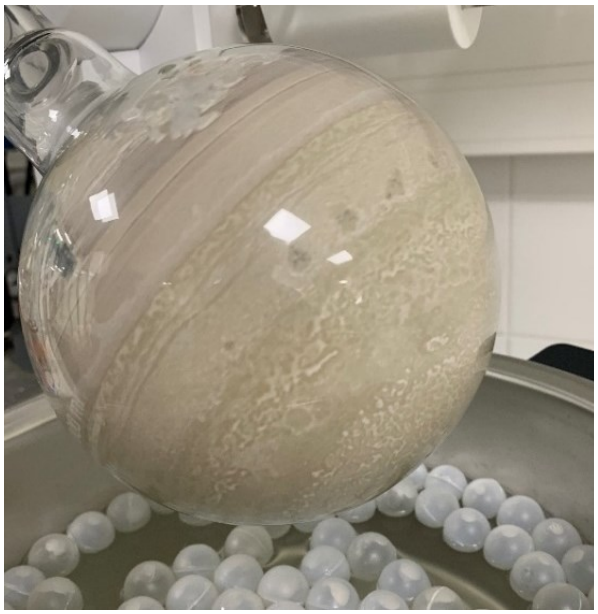

Figure 15. Catalyst drying in the rotary evaporator.

The calcination was conducted with a ramp increase of 1.33 °C/min up to 600°C and then it was kept at that temperature for four hours with a subsequent slow temperature decrease to the ambient one. Such slow temperature increase had the purpose to avoid damage like fractures in the catalyst structure. This process had the objective to decompose the salt to create a tin oxide layer and to fix it on the support surface. After calcination, the catalyst was weighted and measured for a batch experiment.

With Sn-Al_2O_3 catalyst, having 5% of tin, the succinic acid selectivity reached ca 20% (Figure 16) while for maleic acid selectivity got to ca 6%.

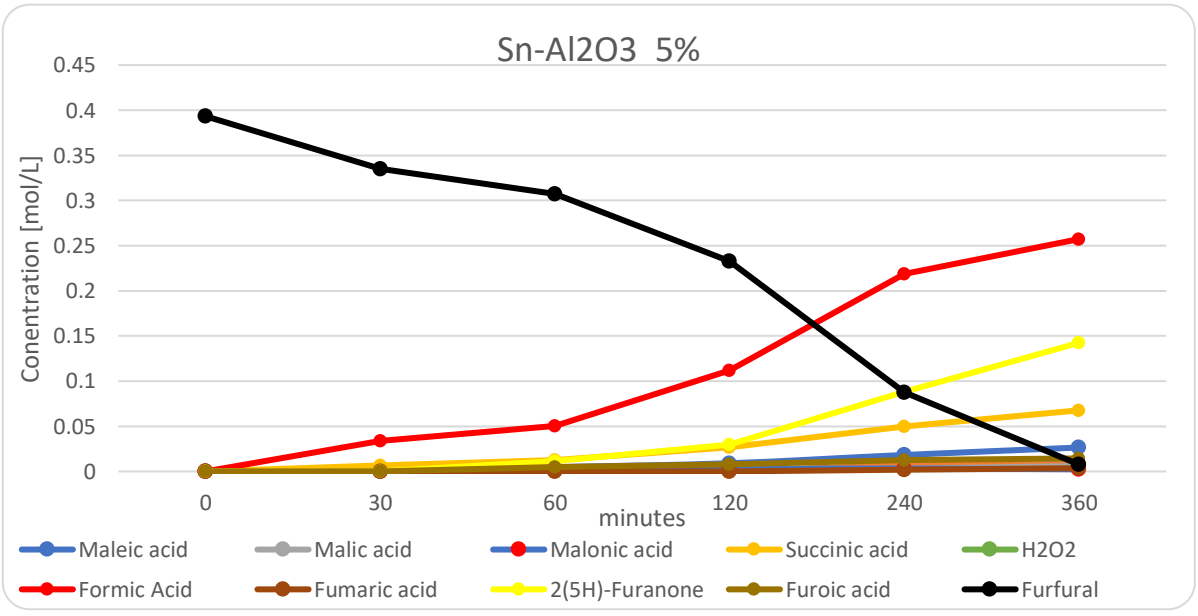

Figure 16. Concentration profiles in furfural oxidation with H_2O_2 over Sn-Al_2O_3 at 5% tin. (Batch, 80°C, 6 h, 700 rpm)

After this experiment, the catalyst was prepared again, but this time adding more tin to it. Keeping 10 g of alumina, 8 g of tin chloride were added following the method explained above, in this way 2.5 g of tin would be present on the catalyst. The result was almost the same as the experiment conducted with 0.5 g. The concentration profiles can be seen in Figure 17.

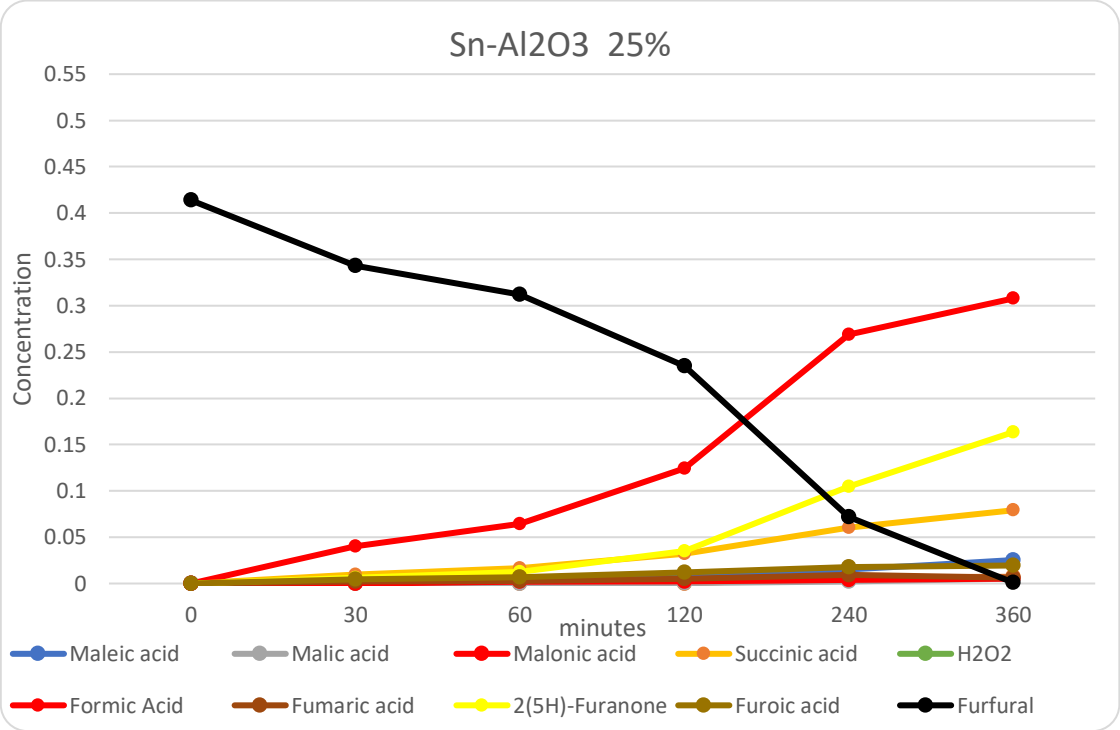

Figure 17. Concentration profiles in furfural oxidation with H_2O_2 over Sn-Al_2O_3 at 25% tin. (Batch, 80°C, 6 h, 700 rpm)

It can be observed from Figure 17 that selectivity towards maleic and succinic remained the same as for the previous case.

Titanium silicalite zeolite Ti-MWW has been reported in literature to have good properties in reactions with hydrogen peroxide [26]. Being similar to TS-1, with different microscopic structures of the channels, the catalyst also displayed low selectivity towards both desired products. It is visible from the concentration profiles of Figure 18 that it promotes formation of formic acid.

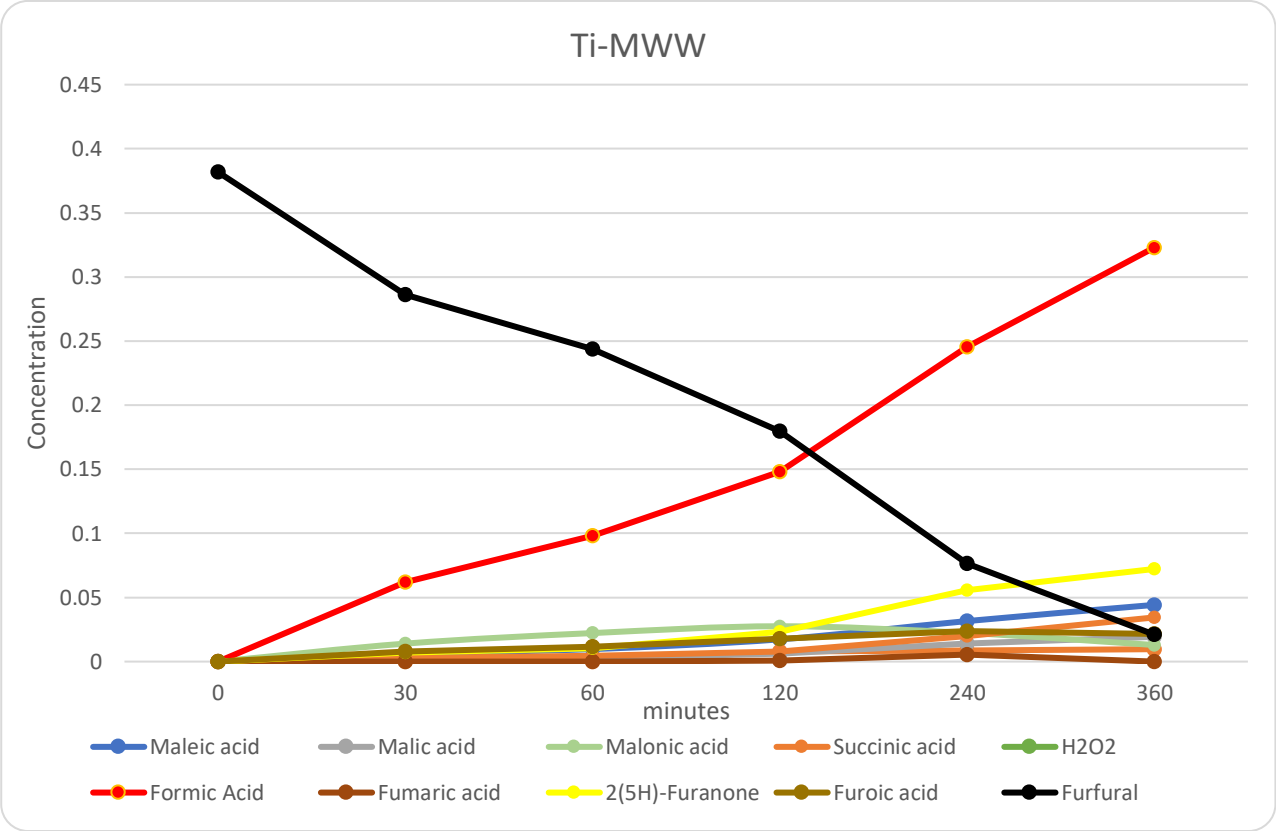

Figure 18. Concentration profiles in furfural oxidation with H_2O_2 over Ti-MWW. (Batch, 80°C, 6 h, 700 rpm)

None of the catalysts described in this section showed any relevant selectivity towards succinic acid, even though they exhibited an acidic structure. It can be thus suggested that the sulfonic groups are the key in achieving high selectivities to succinic and maleic acids. Future laboratory experiments in the laboratory will screen graphene and silica with sulfonic groups attached to them.

Alternatively, sulfuric acid in the liquid state can be used as an efficient catalyst, acting as a homogeneous catalyst with subsequent separation problems. Furthermore, in case of scale up, also more expensive construction materials must be used to prevent corrosion, and more stringent safety measures should be taken. For these reasons there is usually an interest to study and develop efficient heterogeneous catalysts.

2.7 Residence time distribution

To understand how the reactor was working, the residence time distribution experiments were performed with Naftol yellow, an UV reflective colorant. The results of these experiments provided the mean residence time, the average velocity, and the axial dispersion coefficient, which are important parameters used in the balance equations.

The setup for these experiments consisted of two small vessels, one with pure water and the other one with a yellow colorant dissolved in water. A selective valve was placed between the two streams from the vessels and the line to the pump. In this way, only one of the two liquids could be chosen at the time. The pump sent the liquid at the bottom of the PBR and in the outlet a splitter was placed to send a small amount of the liquid to an UV detector and the rest of the liquid to a waste container. This setup allowed a uniform profile of the colorant intensity at the outlet. The standard colorant solution was also analysed to get the steady state value of the colorant intensity.

In Figure 20, the sets of experiments conducted for the three flowrates (ml/min) as a function of time (s) is shown.

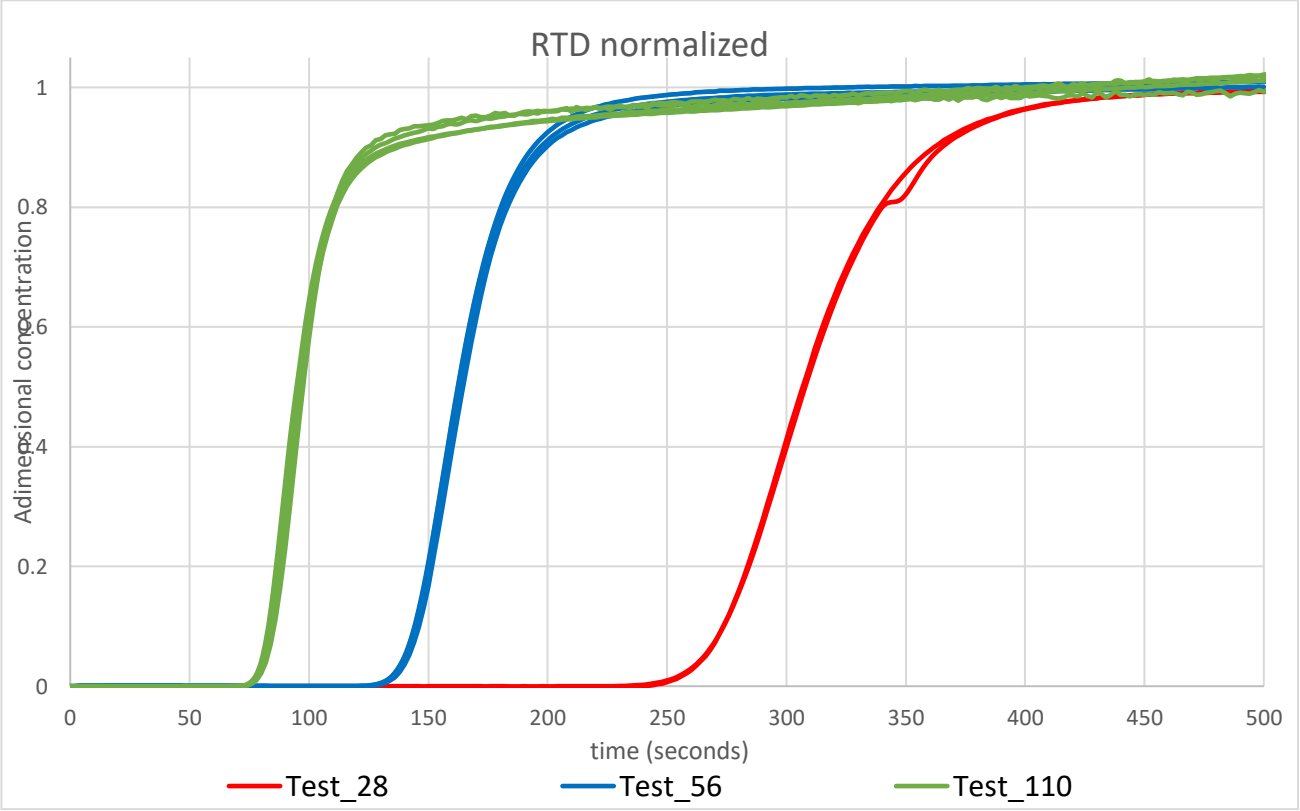

Figure 20. Multiple cumulative response curve versus time for each flow rate used.

For each flow rate used, the average in concentration of the experiments performed was calculated to obtain a representative curve to use in the following analyses.

In Figure 21, the results for the three flow rates of recirculation used are shown, with the outlet concentration normalized as the concentration at dimensionless time θ divided by the concentration of the initial colorant solution, giving the cumulative function F(t).

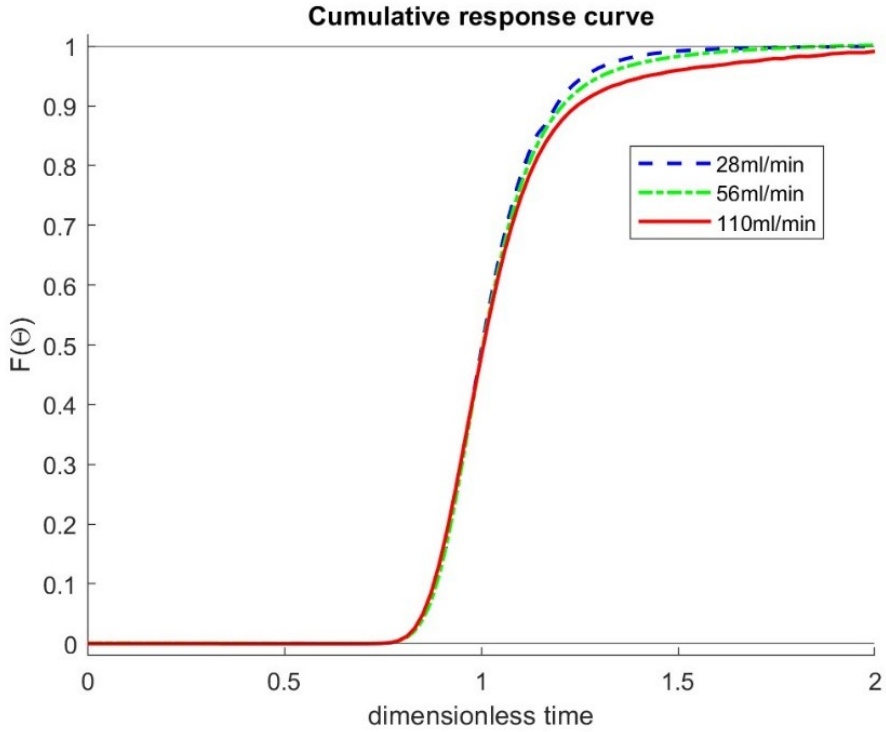

Figure 21. Cumulative response curve versus dimensionless time.

From the data of the cumulative response, it was possible to obtain the profile of E(t) using numerical derivation in MATLAB. E(t) is the residence time distribution function, and it indicates the age distribution of the fluid, which is obtained from the first derivative of F(t). After normalizing, the data profile of E(θ) is fitted with the following equation [28]:

$$E_\theta = \frac{1}{\sqrt{4\pi\left(1/Pé\right)}} \exp\left[-\frac{\left(1-\theta^2\right)}{4\left(1/Pé\right)}\right] \tag{1}$$

This correlation is useful because it allows to obtain the Péclet using it as the variable for the fitting.

The axial dispersion coefficient D is typical of a packed bed reactor, and it will be later used in the balance equations, it represents the degree of back-mixing during the flow. Knowing the velocity of the liquid u, the length of the reactor L, and the Pé number obtained from the fitting, it is possible to calculate the axial dispersion coefficient D:

$$Pé = \frac{uL}{D} = \frac{advective\ transport\ rate}{dispersive\ transport\ rate} \tag{2}$$

In Figure 22, a comparison between the E(θ) obtained experimentally for the flow rate of 56 ml/min and E(θ) functions for different values of Péclet number is given.

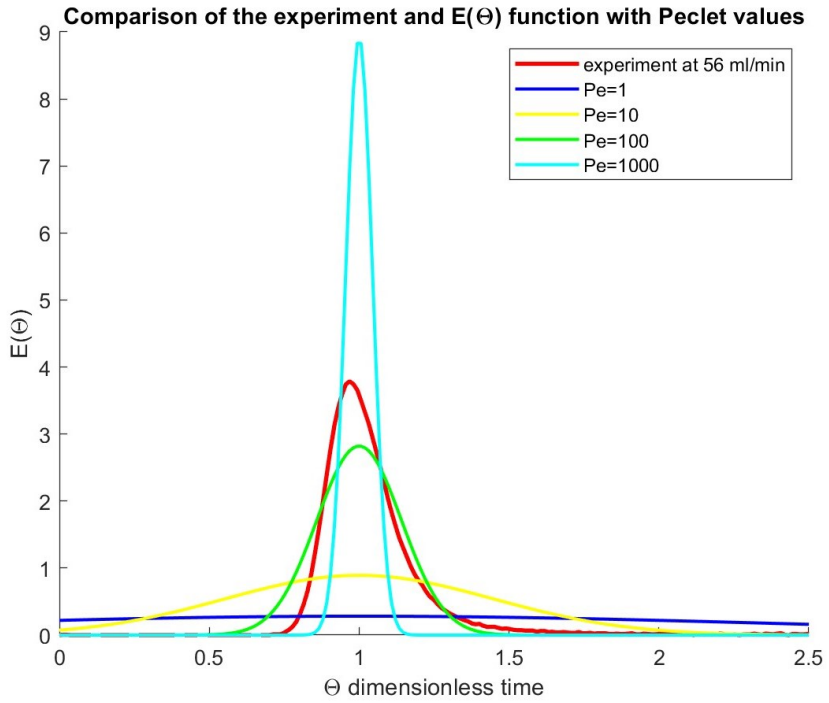

Figure 22. Residence time distribution function.

In Table 5, the three values of Péclet number and axial dispersion coefficient are shown for each flow rate.

Table 5, Axial dispersion parameters.

Flow rate (ml/min)	28	56	110
Velocity (cm/s)	0.213	0.4175	0.8202
Péclet number	204	195	175
Axial dispersion coefficient (m^2/s)	$5.47*10^{-6}$	$1.12*10^{-5}$	$2.50*10^{-5}$
Mean residence time (s)	239	122	62

An ideal plug flow reactor is reached when the E(θ) function has a single pulse shape, hence when Pe → ∞. As an approximation, it is usually accepted to use the PFR model when the value of the Peclet number is larger than 100.

CHAPTER 3
KINETIC MODELLING

3.1 Model assumptions and fitting descriptors

During the experiments the samples were withdrawn at the outlet of the packed bed reactor, and at the outlet of the mixing tank (Figure 46). Plotting these concentrations versus time, very similar values in the profiles at the two outlets were noticed. Therefore, it was concluded that no reactions took place in the mixing tank. In addition, the concentrations downstream of the PBR, had a fluctuating behaviour, for example with small jumps in the concentration values, resulting in not so smooth profiles for most of the components. For this reason, it was decided to only consider the concentrations values out of the mixing tank for the fitting process.

Since the concentrations in the two measurements points, at the inlet and outlet of the mixing tank, were very similar, it was decided to remove the mixing tank from the model and add a time delay. In this way, the assumption was made of a long tube which takes into account the residence time of the mixing tank being directly connected to the inlet of the PBR (Figure 47).

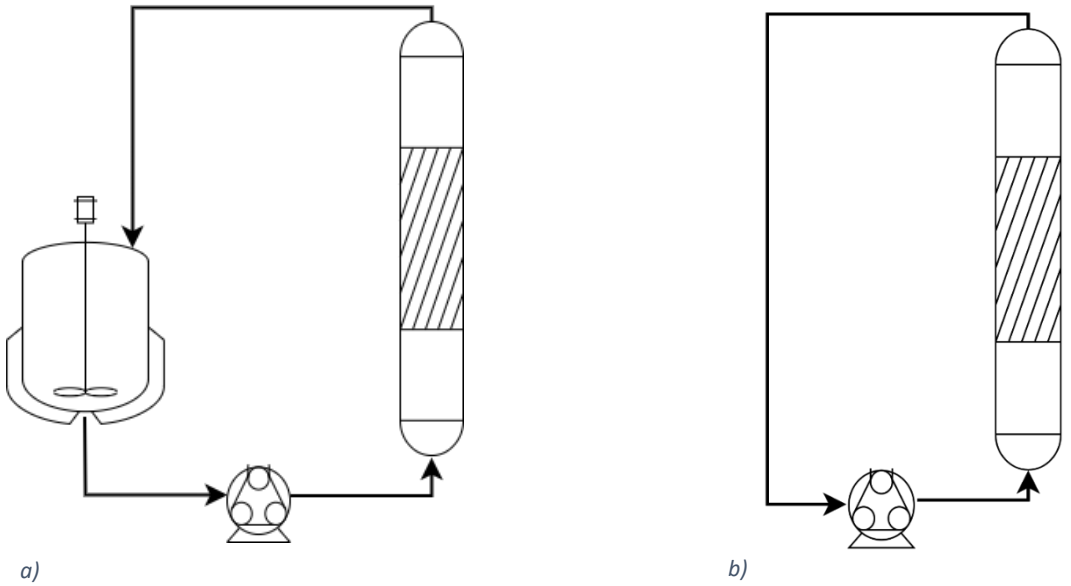

Figure 46. Reactor setup (a) with a mixing tank, (b) approximated with a longer tube.

To measure the quality of the fitting of the various reaction mechanism considered, two statistical parameters were used. The first one is the coefficient of determination R^2, which indicates how well the model fits the experimental data.

The coefficient of determination is defined as:

$$R^2 = \left(1 - \frac{SS_{res}}{SS_{tot}}\right) * 100 \tag{5}$$

where SS_{res} is the sum of the residuals squared, while SS_{tot} is the total sum of squares and are calculated as shown in Eq 6.

$$SS_{res} = \sum_i (y_i - f_i)^2 \qquad SS_{tot} = \sum_i (y_i - \overline{y_i})^2 \tag{6}$$

Where *f* stands for the calculated concentration values and *y* the experimental ones.

The second descriptor is the relative error for the concentrations, which is defined as

$$E_{rel} = \frac{\left|C_{calc} - C_{\exp}\right|}{C_{\exp}} * 100 \tag{7}$$

3.2 Mathematical model of a packed bed reactor operated in a closed loop system

At the beginning a simple batch reactor model was used to practice with the parameter estimation code in MATLAB. Furthermore, this model is a simplification of the whole apparatus because the reagents are introduced in the system and then reacted, without any addition or removal. The batch reactor model applied for the initial fitting was:

$$\frac{\partial C_i}{\partial t} = r_i \tag{8}$$

The fitting using the batch reactor model gave R^2 of the 88.6% and a relative error of 20.6%.

In the next stage, a more detailed model was implemented. To describe the experiments with the flow rate variations to be mathematically included in the mass balance.

Since the Peclet number was higher than 100 for all the three flow rates used, a plug flow reactor model with recycle could in principle be used to describe the reactor with sufficient precision. It was decided however, for the sake of a more general treatment, to use the material balance for a packed bed reactor with axial dispersion. The axial dispersion coefficient D_z and the average velocity u were estimated from the RTD experiments using the correlations from the literature [27-28]. The use of such model improved the fitting results, initially increasing R^2 to 94.3%. Then, after many iterations of the parameter estimation code, the best combination of K and E_a were found for each reaction, resulting with R^2 of 96.3% and the relative error of the concentrations of 15.1%.

The mass balance for a packed bed reactor with axial dispersion used for the final fitting process is shown in Eq.8:

$$\frac{\partial C_i}{\partial t} = -u\frac{\partial C_i}{\partial z} + D_z\frac{\partial^2 C_i}{\partial z^2} + \sum_{j=1}^{N_r}\nu_{ij}r_j\rho_B \tag{9}$$

The term on the left-hand side represents the accumulation, the second term indicates the variation in the concentration due to the convection and the third one describes the axial dispersion due to the effect of the packing with the flow. Lastly, the term on the right-hand side represents the production or consumption of a component *i* in a reaction j.

Equation 8 was applied using the backward difference method to discretize the reactor length z.

According to the Weisz-Prater criterion in Eq. 9 [33], limitations in the intraparticle diffusion can be neglected if $C_{W\text{-}P}$ is less than 1.

$$C_{W-P} = \frac{-r_{obs}\rho_p R_p^2}{D_{e,Fu}\rho_B C_{Fu,0}} \tag{10}$$

where r_{obs} is the observed reaction rate [mol/(m^{3}s)], ρ_p is the catalyst density [kg/m^3], R_p the radius of the catalyst particles [m], $D_{e,\,Fu}$ is the effective diffusion coefficient [m^2/s], ρ_B is the bulk density of the reactor [kg/m^3], and $C_{Fu,0}$ is the initial concentration of furfural [mol/m^3]. Eq. 9 resulted to be less than 1, mainly due to the low rate of the reaction, allowing to neglect the intra-particle diffusion.

In the presence of a heterogeneous catalytic reaction, three processes take place: adsorption, surface reaction and desorption. Typically, one of the previous mechanisms is usually rate-limiting. In the example of ammonia production, in the Haber-Bosch process, nitrogen and hydrogen gas are made to react over iron oxides. The surface reaction is very fast and the residence time in the reactor is in the order of few seconds, for this reason, such reaction is an example of adsorption as the limiting step [32]. For furfural oxidation with hydrogen peroxide on Amberlyst-15, many hours are required to obtain substantial yields of the products and the residence time in the reactor are in the order of few minutes. For this reason, the approximation of the reaction rate as limiting step is made, and the terms representing the adsorption-desorption are neglected.

The rate equations for each component according to the reaction network of Figure 47 are written as

$$r_{Fu} = -k_{21}C_{Fu}C_{H_2O_2} - k_{10}C_{Fu}C_{H_2O_2} \tag{11}$$

$$r_{Int9} = k_{21}C_{Fu}C_{H_2O_2} - k_3C_{Int9}\rho_B - k_1C_{Int9} \tag{12}$$

$$r_{Int19} = k_3C_{Int9} - k_{17}C_{Int19} \tag{13}$$

$$r_{Int14} = k_1 C_{Int9}^{n} + k_4 C_{2(3H)F} - k_{14} C_{Int14} C_{H_2O_2} - k_2 C_{Int14} C_{H_2O_2} - k_{19} C_{Int14} \quad (14)$$

$$r_{2(5H)F} = k_{17} C_{Int19} + k_{24} C_{2(3H)F} - k_{23} C_{2(5H)F} \quad (15)$$

$$r_{MaloAcid} = k_{14} C_{Int14} C_{H_2O_2} - k_{13} C_{MaloAcid} C_{H_2O_2} \quad (16)$$

$$r_{2(3H)F} = -k_{24} C_{2(3H)F} + k_{23} C_{2(5H)F} - k_4 C_{2(3H)F} + k_{19} C_{Int14} - k_5 C_{2(3H)F} \quad (17)$$

$$r_{Int15} = k_2 C_{Int14} C_{H_2O_2} - k_{22} C_{Int15} \quad (18)$$

$$r_{5h2(5H)F} = k_{22} C_{Int15} - k_6 C_{5h2(5H)F} C_{H_2O_2} \quad (19)$$

$$r_{FurAcid} = k_{10} C_{Fu} C_{H_2O_2} \quad (20)$$

$$r_{Int16} = k_5 C_{2(3H)F} - k_7 C_{Int16} C_{H_2O_2} \quad (21)$$

$$r_{SAcid} = k_7 C_{Int16} C_{H_2O_2} \quad (22)$$

$$r_{MaleAcid} = k_6 C_{5h2(5H)F} C_{H_2O_2} + k_{18} C_{FumAcid} - k_8 C_{MaleAcid} - k_{15} C_{MaleAcid} - k_{20} C_{MaleAcid} C_{H_2O_2} \quad (23)$$

$$r_{FumaAcid} = k_8 C_{MaleAcid} - k_{18} C_{FumAcid} - k_{11} C_{FumAcid} \quad (24)$$

$$r_{MaliAcid} = k_{15} C_{MaleAcid} + k_{11} C_{FumAcid} - k_{12} C_{MaliAcid} C_{H_2O_2} \quad (25)$$

$$r_{TarAcid} = k_{20} C_{MaleAcid} C_{H_2O_2} - k_{25} C_{TarAcid} C_{H_2O_2} \quad (26)$$

$$r_{FormAcid} = k_1 C_{Int9} + k_{17} C_{Int19} - k_9 C_{FormAcid} C_{H_2O_2} \quad (27)$$

$$r_{H_2O_2} = -k_6 C_{5h2(5H)F} C_{H_2O_2} - k_7 C_{Int16} C_{H_2O_2} - k_9 C_{FormAcid} C_{H_2O_2} - k_{10} C_{Fu} C_{H_2O_2} - k_{12} C_{MaliAcid} C_{H_2O_2} \quad (28)$$
$$- k_{13} C_{MaloAcid} C_{H_2O_2} - k_{14} C_{Int14} C_{H_2O_2} - k_{16} C_{H_2O_2} - k_{20} C_{MaleAcid} C_{H_2O_2} - k_{21} C_{Fu} C_{H_2O_2} - k_{25} C_{TarAcid} C_{H_2O_2}$$

were *Fu* stands for furfural, H_2O_2 for hydrogen peroxide, *MaloAcid* is malonic acid, *2(5H)F* is 2(5H)furanone, analogous for 2(3H)furanone and 5-hydroxy-2(5H)-furanone. *MaleAcid* is maleic acid, *SAcid* is succinic acid, *FumaAcid* is fumaric acid, *MaliAcid* is malic acid, *FormAcid* is formic acid and *TarAcid* is tartaric acid.

Several unstable intrmediates (*Int*) are also presented in the reaction scheme. *Int9* is furfural-α-hydroxy-hydroperoxide, *Int19* is furan-2-yl hydrogen carbonate, *Int14* is 2-hydroxyfuran, *Int15* is 4-hydroperoxycyclopent-2-en-1-ol and *Int16* is (E)-4-hydroxybut-3-enoic acid.

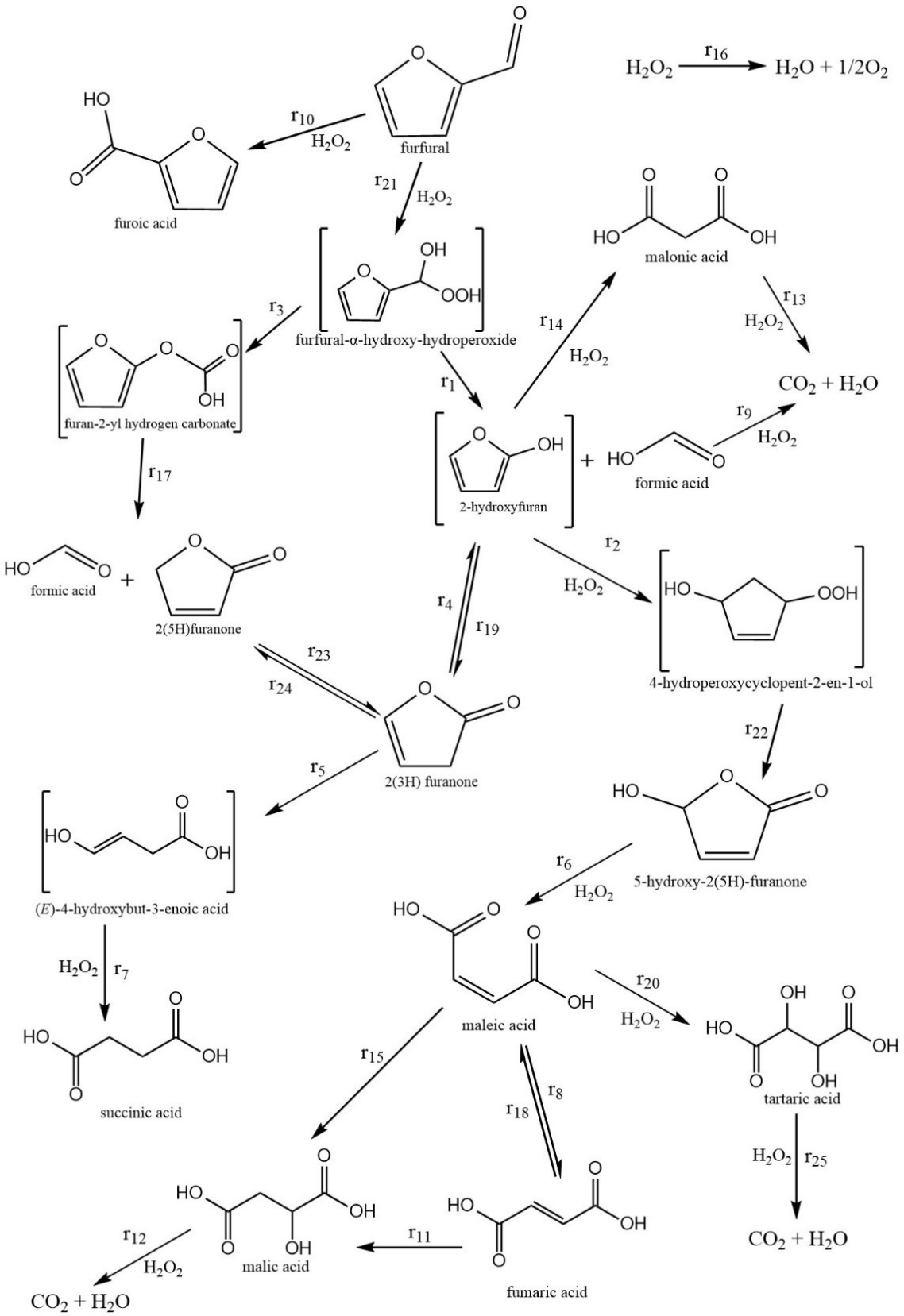

Figure 47. The modified reaction network.

For each reaction two parameters were estimated, the kinetic constant at the reference temperature and the activation energy.

In the iteration process written in MATLAB, initial estimations of k_n and $E_{a,n}$ were guessed and used as the starting point to find the optimal combination for each rate constant as shown in Eq. 28. The subscript n indicates the reaction, and i is the iteration number.

$$k_{n,i} = k_{n,i-1} e^{\left(-\frac{E_{a,n}}{R} \left(\frac{1}{T} - \frac{1}{T_{avg}} \right) \right)} \tag{29}$$

All the experiments were fitted simultaneously, to calculate the objective function and refine the values of the 50 parameters. The objective function used to reach the best fit was defined by Eq. 29:

$$U = \sum_{j=1}^{N_r} \sum_{i=1}^{N_c} (C_{ij}^{calc} - C_{ij}^{\exp})^2 \tag{30}$$

Where the indices j stands for the experiment in consideration, while i indicates the component.

The `lsqnonlin` solver was used for the fitting, first applying the `trust-region-reflective` algorithm, and then close to the solution the `levenberg-marquardt` was used.

3.3 Results of data fitting

3.3.1 Fitting profiles

The fitting results using the axial dispersion model for the packed bed reactor are shown in Figure 48 and 49. For the sake of clarity in Figure 48 only the most relevant compounds are shown, with *furfural* in black, formic acid in red, *2(5H)-furanone* in light blue, *succinic acid* in orange, *2(3H)-furanone* in purple and *maleic acid* in blue.

In particular, furfural is consumed, and formic acid formed as a prominent stoichiometric co-product in many reactions. *2(3H)-furanone* is the intermediate responsible for the production of *succinic acid*, being initially formed and then consumed, while *2(5H)-furanone* is the unreactive isomer. Finally, *maleic acid* is the other product of interest being produced in smaller quantities from *5-hydroxy-2(5H)-furanone*.

The dots in these plots represent the experimental values of the concentrations expressed in mol/L, and the curves are the result of the fitting obtained with the balance equations.

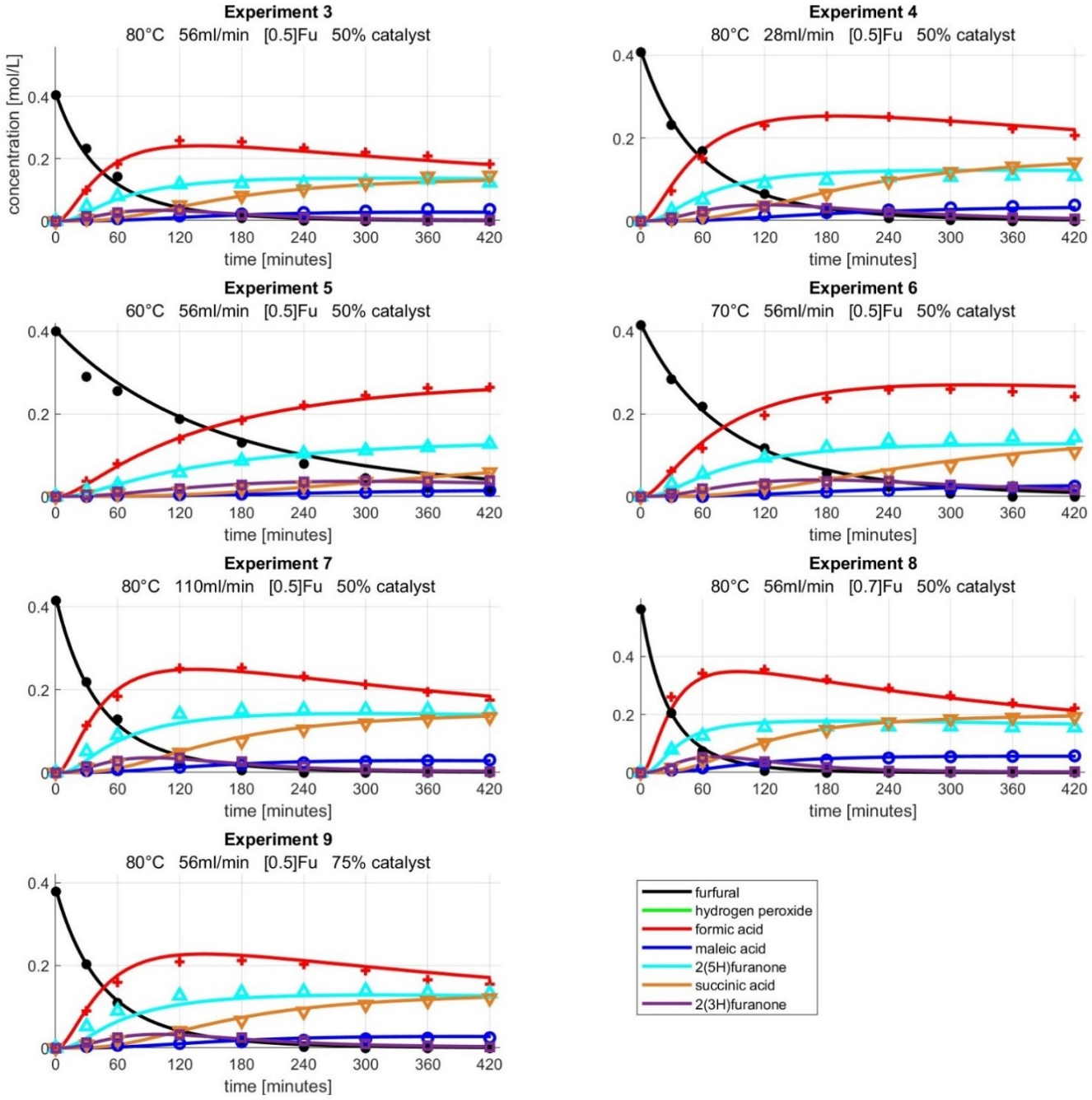

Figure 48. Fitting results for the main components.

In the following series of plots, hydrogen peroxide is shown and marked with green points and curve.

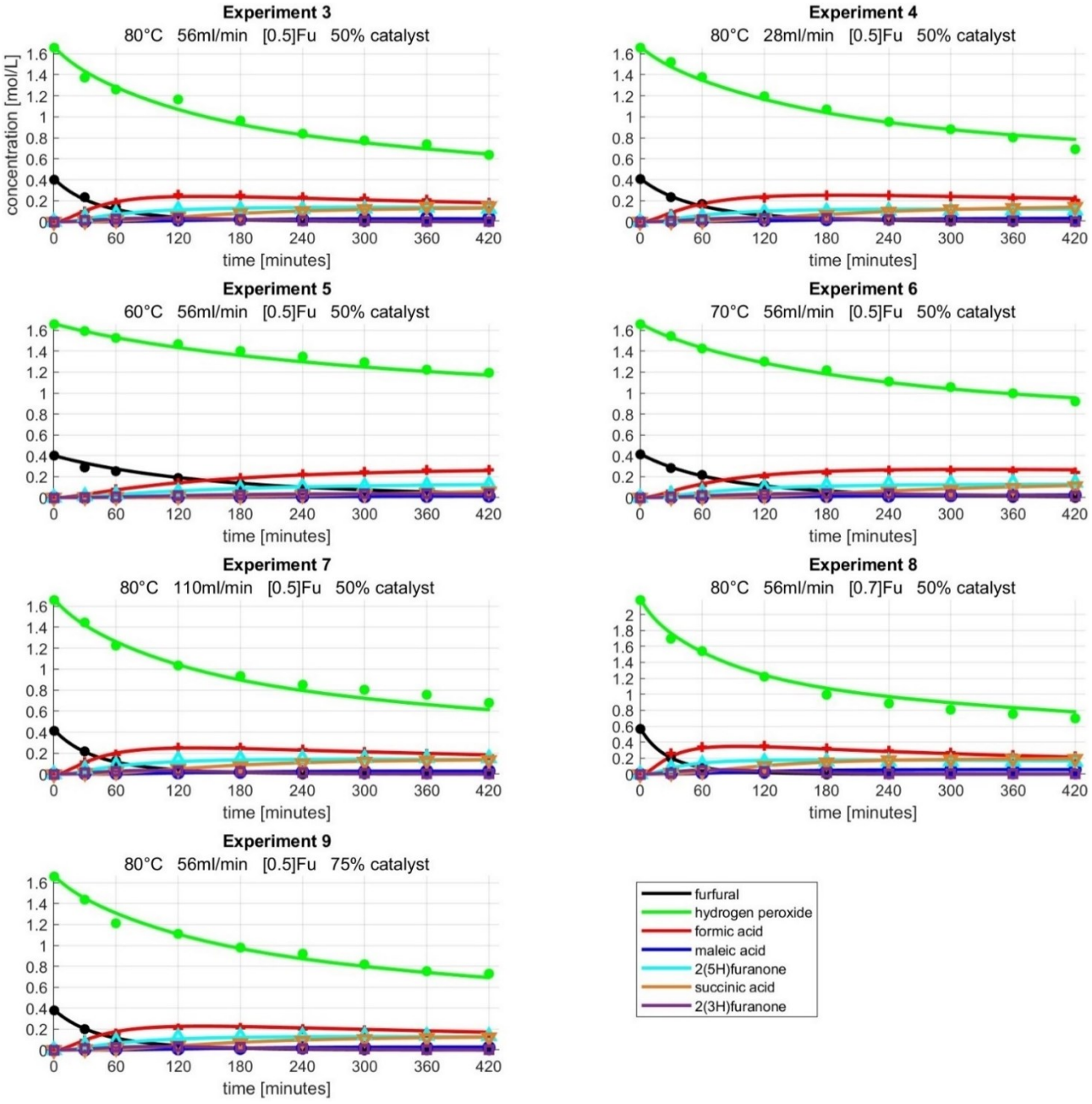

Figure 49. Fitting results for the main components with hydrogen peroxide.

From the two images of the fitting, it can be concluded that the mechanism identified in Figure 47 is representative for the reactions occurring in the furfural oxidation with hydrogen peroxide over Amberlyst-15.

3.3.2 Estimated parameters

All the 50 estimated parameters are shown in Table 19, 25 of them are activation energies while 25 are kinetic constants at the reference temperature.

Table 19. Estimated parameters values.

Activation Energy						
Parameter	Ea_1	Ea_2	Ea_3	Ea_4	Ea_5	Ea_6
Units	J/mol	J/mol	J/mol	J/mol	J/mol	J/mol
Value	6˙100	48˙600	1˙000	36˙100	51˙100	1˙000
Parameter	Ea_7	Ea_8	Ea_9	Ea_{10}	Ea_{11}	Ea_{12}
Units	J/mol	J/mol	J/mol	J/mol	J/mol	J/mol
Value	1˙000	1˙000	104˙200	46˙000	796˙900	113˙800
Parameter	Ea_{13}	Ea_{14}	Ea_{15}	Ea_{16}	Ea_{17}	Ea_{18}
Units	J/mol	J/mol	J/mol	J/mol	J/mol	J/mol
Value	81˙700	49˙000	114˙900	129˙400	2˙800	113˙900
Parameter	Ea_{19}	Ea_{20}	Ea_{21}	Ea_{22}	Ea_{23}	Ea_{24}
Units	J/mol	J/mol	J/mol	J/mol	J/mol	J/mol
Value	32˙600	146˙300	54˙700	1˙000	63˙100	363˙300
Parameter	Ea_{25}					
Units	J/mol					
Value	356˙700					

Kinetic constants						
Parameter	K_1	K_2	K_3	K_4	K_5	K_6
Units	min^{-1}	L/(mol*min)	min^{-1}	min^{-1}	min^{-1}	L/(mol*min)
Value	0.5428	0.0486	0.4586	0.0924	0.2533	0.1835
Parameter	K_7	K_8	K_9	K_{10}	K_{11}	K_{12}
Units	L/(mol*min)	min^{-1}	L/(mol*min)	L/(mol*min)	min^{-1}	L/(mol*min)
Value	1.0261	0.0337	0.0196	0.0413	0.1074	1.3000
Parameter	K_{13}	K_{14}	K_{15}	K_{16}	K_{17}	K_{18}
Units	L/(mol*min)	L/(mol*min)	min^{-1}	min^{-1}	min^{-1}	min^{-1}
Value	0.0255	0.0068	0.0001	0.0066	0.6276	0.4655
Parameter	K_{19}	K_{20}	K_{21}	K_{22}	K_{23}	K_{24}
Units	min^{-1}	L/(mol*min)	L/(mol*min)	min^{-1}	min^{-1}	min^{-1}
Value	0.2470	0.0001	0.1509	1.3002	0.0119	0.0413
Parameter	K_{25}					
Units	min^{-1}					
Value	0.0001					

As visible in Table 19, some values of the activation energies are low since they represent reactions from unstable intermediates to stable products, in addition, also the pre-exponential factors show high values, indicating the rapidity of such reactions.
An example of instantaneous reaction in this study is from (E)-4-hydroxybut-3-enoic acid to succinic acid (reaction r_7 in Figure 47).

Parameter estimation, aimed at determining pre-exponential factors and activation energies is finalized at the design simulation and optimization of an industrial reactor [34].

3.3.3 Statistical analysis

Parity plots

The parity plots in Figure 50, show the ±10% confidence interval which is delimited by the two green lines and the ±20% interval drawn in blue. Almost all the points representing the main components are within this interval apart from *2(3H)-furanone* which is less well described. The reason for that might be that the calibration for this compound was not known, and the data for *2(5H) furanone* were used instead.

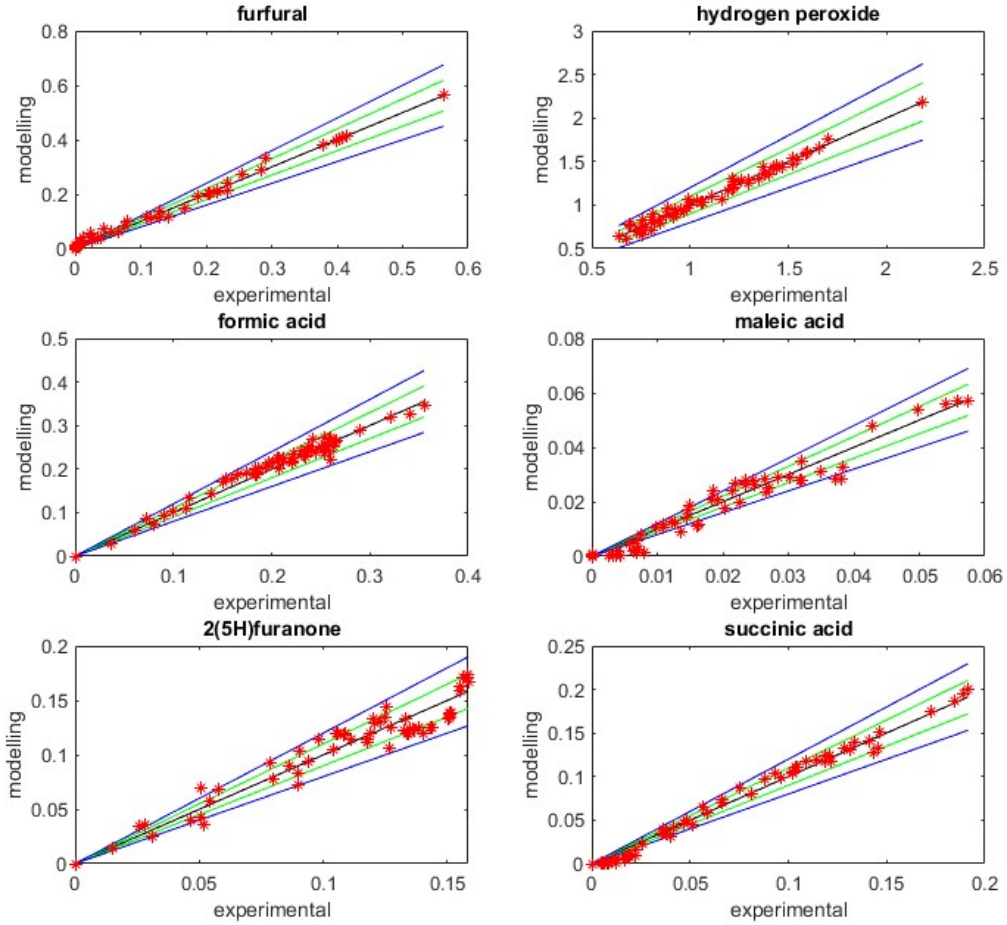

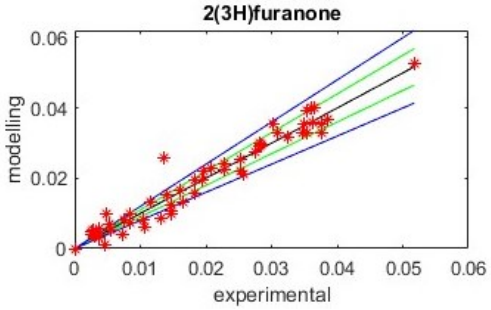

Figure 50. Parity plot of the main components.

Contour plots

Few reactions, responsible for the production of the main intermediates and products, accordingly to the scheme in Figure 47, were considered to perform a sensitivity analysis on the estimated parameters.

As shown in the contour plots in Figure 51, the activation energy is given on the y-axis, while the kinetic constants are on the x-axis. In the z-axis, is the value of R^2 and the contour lines define the areas with equal values.

Few contour plots for the most important reactions are displayed in Figure 51.

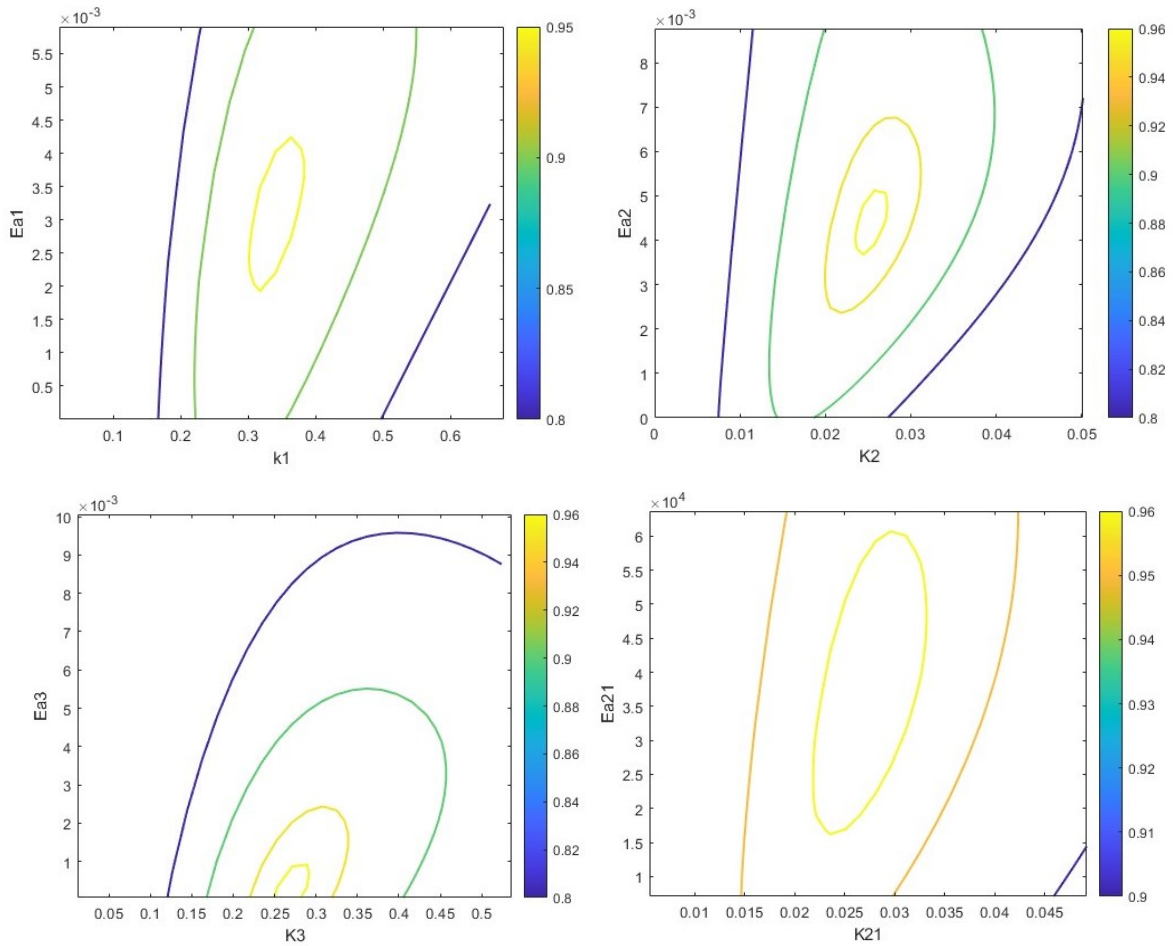

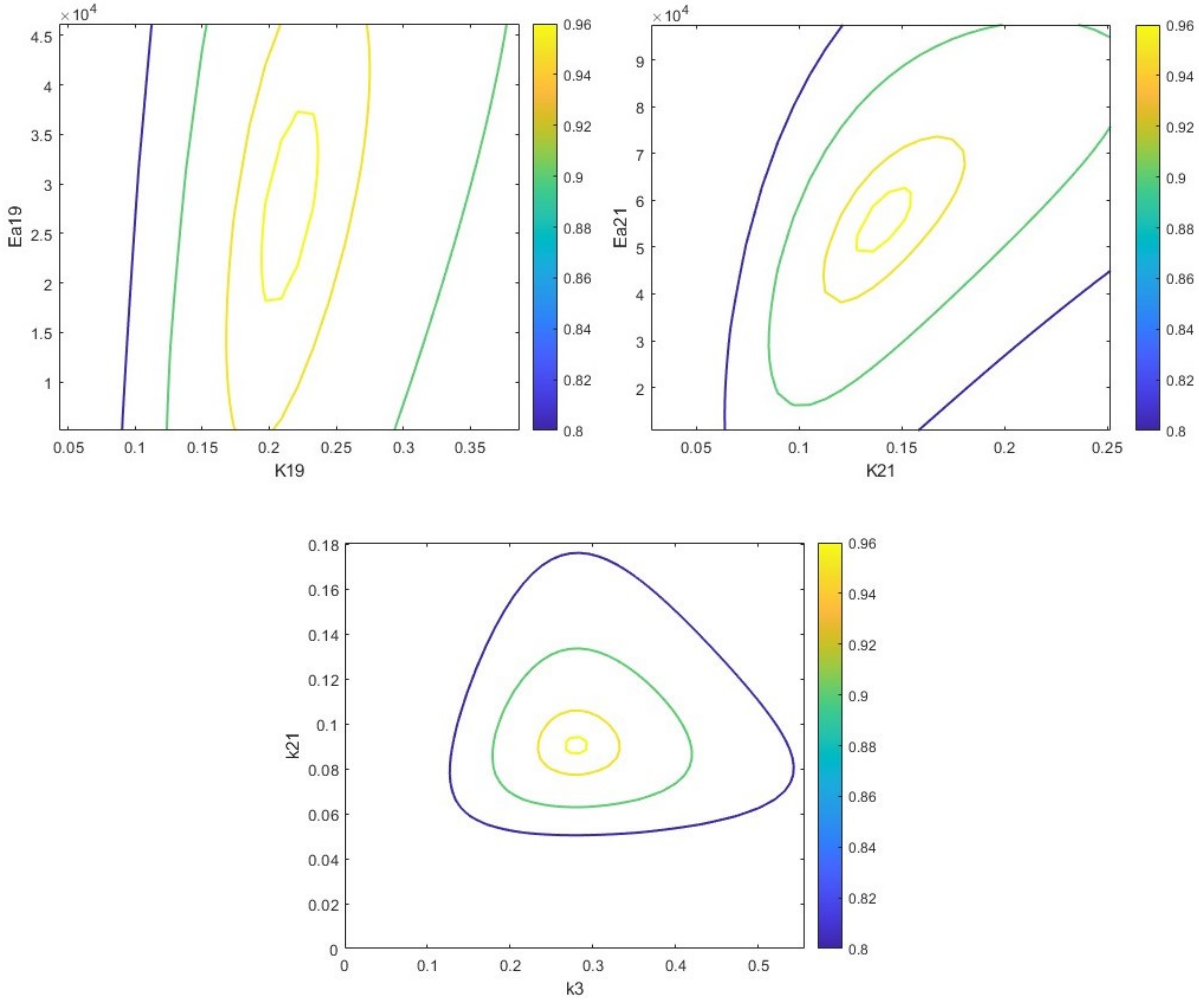

Figures 51. Contour plots for the main parameter pairs.

From these contour plots, the area inside the yellow curve indicates where the couple of parameters will give an R^2 higher than 96%. The goal with these plots is to show the low dependency of the activation energy from the kinetic constants at the reference temperature for the most relevant reactions. Furthermore, only in a restrict range of the parameters pair it is possible to obtain R^2 value exceeding 96%.

CONCLUSIONS AND FUTURE PRESPECTIVES

The aim of the study of furfural oxidation on a heterogeneous catalyst was to investigate the use of Amberlyst-15 to produce succinic and maleic acid. Furthermore, a better understanding of the reaction mechanism was necessary to describe the profiles of all the compounds appearing during the reaction time. Finally, there was also the interest to understand if a packed bed reactor operated at full recycle could offer a promising solution to conduct slow reactions.

All the major components formed, and most of the ones in low concentrations were identified, leading to a hypothesis of a reaction route through which succinic acid is formed from 2(3H)-furanone. Unfortunately, due to instability of 2(3H)-furanone, it was not possible to test it in a small batch reactor to prove formation of succinic acid. A more detailed study, focused on this molecule, can lead to isolation, testing and analysis of it and its products.

As result of the experiments with furfural and with the reaction intermediates, an improved reaction network was presented, and it was used to write the component mass balance equations for the fitting of the experimental data. In the data fitting process, the twenty-five reactions identified were used and the respective activation energy and pre-exponential factors were estimated by non-linear regression analysis. The quality of the fitting was measured with degree of determination (R^2) and the relative error, reaching 96.3% and 15.1%, respectively.

This work has also highlighted the behaviour of Amberlyst-15 in the presence of water and under acidic conditions. The advantages and disadvantages of using a polymer-supported acid catalyst as Amberlyst-15 were investigated. As a result, solutions to breakage of the catalyst and reactor occlusion were described, and alternative catalysts such as graphene and silica with sulfonic groups were proposed with the aim of eliminating the problem of swelling and breakdown of the catalyst at the reaction conditions.

Finally, the use of a setup composed by a packed bed reactor operated at the full recycle mode proved to be reliable and convenient when dealing with slow reactions, to have a fixed and low amount of solid catalyst available. If a faster production is required, the ratio of catalyst amount over reactor volume could be increased and the ratio of catalyst amount over liquid reactants volume.

A useful investigation should focus on limiting production of 2(5H)-furanone or to transform it into other useful products, since at the moment this compound represents merely a significant undesired side product in furfural oxidation.

NOTATION

C_i = concentration of species *i*

D_z = axial dispersion coefficient

E_{rel} = relative error

E(t) = residence time distribution function

E(θ) = dimensionless residence time distribution function

F(t) = cumulative residence time distribution function

HPLC = High Performance Liquid Chromatography

k_i = kinetic constant of reaction *x*

PBR = packet bed reactor

Pé = Péclet number

r_i = reaction rate of reaction *i*

R = gas constant

R^2 = coefficient of determination

S_x = selectivity of the product x from furfural

t = time

T_{avg} = average temperature

u = velocity of the liquid in the packed bed reactor

USD = United States Dollar

UV = ultraviolet

z = reactor length coordinate

θ = dimensionless time

v = stoichiometric coefficient

ρ_B = reactor catalyst density

REFERENCES

[1] Glavič, P., Pintarič, Z. N., Levičnik, H., Dragojlović, V. & Bogataj, M. Transitioning towards Net-Zero Emissions in Chemical and Process Industries: A Holistic Perspective. *Processes* **11**, 2647 (2023).

[2] https://mmm.fi/en/forests/use-of-wood

[3] Luque, R. Catalytic chemical processes for biomass conversion: Prospects for future biorefineries. *Pure and Applied Chemistry* **86**, 843–857 (2014).

[4] Heterogeneous Catalytic Oxidation of Furfural with Hydrogen Peroxide over Sulfated Zirconia. *Ind. Eng. Chem. Res.* **59**, 13516–13527 (2020).

[5] Saleem, F. *et al.* Kinetics and modelling of furfural oxidation with hydrogen peroxide over a fibrous heterogeneous catalyst: effect of reaction parameters on yields of succinic acid. *Journal of Chemical Technology & Biotechnology* **92**, 2206–2220 (2017).

[6] Lou, Y., Marinkovic, S., Estrine, B., Qiang, W. & Enderlin, G. Oxidation of Furfural and Furan Derivatives to Maleic Acid in the Presence of a Simple Catalyst System Based on Acetic Acid and TS-1 and Hydrogen Peroxide. *ACS Omega* **5**, 2561–2568 (2020).

[7] da Silva, M. J. & Rodrigues, A. A. Metal silicotungstate salts as catalysts in furfural oxidationreactions with hydrogen peroxide. *Molecular Catalysis* **493**, 111104 (2020).

[8] Choudhary, H., Nishimura, S. & Ebitani, K. Highly Efficient Aqueous Oxidation of Furfural to Succinic Acid Using Reusable Heterogeneous Acid Catalyst with Hydrogen Peroxide. *Chem. Lett.* **41**, 409–411 (2012).

[9] Kingkaew, W., Kaewwiset, T., Thubsuang, U., Siripattana, C. & Nuithitikul, K. Catalytic Oxidation of Furfural to Succinic Acid in the Presence of Sulfonic Resins. *Key Engineering Materials* **856**, 182–189 (2020).

[10] https://pubchem.ncbi.nlm.nih.gov/compound/Furfural

[11] Zhang, L., Xi, G., Yu, K., Yu, H. & Wang, X. Furfural production from biomass–derived carbohydrates and lignocellulosic residues via heterogeneous acid catalysts. *Industrial Crops and Products* **98**, 68–75 (2017).

[12] grandviewresearc.com/industry-analysis/furfural-market

[13] https://pubchem.ncbi.nlm.nih.gov/compound/Hydrogen-Peroxide

[14] https://www.marketsandmarkets.com/Market-Reports/hydrogen-peroxide-market

[15] https://pubchem.ncbi.nlm.nih.gov/compound/Succinic-Acid

[16] grandviewresearc.com/industry-analysis/succinic-acid-market

[17] https://pubchem.ncbi.nlm.nih.gov/compound/Maleic-Acid

[18] https://www.grandviewresearch.com/industry-analysis/malic-acid-market

[19] https://www.shimadzu.com/an/service-support/technical-support/analysis-basics/basic/refractive_index_detection.html

[20] https://www.sigmaaldrich.com/IT/it/product/sial/216380

[21] https://www.dupont.com/content/dam/dupont/amer/us/en/water-solutions/public/documents/en/IER-AmberLyst-15DRY-PDS-45-D00927-en.pdf

[22] Malshe, V. C. & Sujatha, E. S. Regeneration and reuse of cation-exchange resin catalyst used in alkylation of phenol. *Reactive and Functional Polymers* **35**, 159–168 (1997).

[23] https://www.lenntech.com/Data-sheets/Amberlyst-15wet-L.pdf

[24] Lou, Y., Marinkovic, S., Estrine, B., Qiang, W. & Enderlin, G. Oxidation of Furfural and Furan Derivatives to Maleic Acid in the Presence of a Simple Catalyst System Based on Acetic Acid and TS-1 and Hydrogen Peroxide. *ACS Omega* **5**, 2561–2568 (2020).

[25] Lou, Y., Marinkovic, S., Estrine, B., Qiang, W. & Enderlin, G. Oxidation of Furfural and Furan Derivatives to Maleic Acid in the Presence of a Simple Catalyst System Based on Acetic Acid and TS-1 and Hydrogen Peroxide. *ACS Omega* **5**, 2561–2568 (2020).

[26] Wróblewska, A., Makuch, E. & Miądlicki, P. The oxidation of limonene at raised pressure and over the various titanium-silicate catalysts. *Polish Journal of Chemical Technology* 82–87 (2015) doi:10.1515/pjct-2015-0072.

[27] H. Scott Fogler, Elements of Chemical Reaction Engineering, Fourth edition, Prentice Hall 2005

[28] Octave Levenspiel, Chemical Reaction Engineering, Wiley-1999

[29] Palai, Y. N., Shrotri, A. & Fukuoka, A. Selective Oxidation of Furfural to Succinic Acid over Lewis Acidic Sn-Beta. *ACS Catal.* **12**, 3534–3542 (2022).

[30] Li, F., Lu, T., Chen, B., Huang, Z. & Yuan, G. Pt nanoparticles over TiO2–ZrO2 mixed oxide as multifunctional catalysts for an integrated conversion of furfural to 1,4-butanediol. *Applied Catalysis A: General* **478**, 252–258 (2014).

[31] Catalysts | Free Full-Text | Influence of Pd and Pt Promotion in Gold Based Bimetallic Catalysts on Selectivity Modulation in Furfural Base-Free Oxidation. https://www.mdpi.com/2073-4344/11/10/1226.

[32] Ullmann's Encyclopedia of Industrial Chemistry. 6th ed.Vol 1: Federal Republic of Germany: Wiley-VCH Verlag GmbH & Co. 2003 to Present, p. V10 526 (2003)

[33] Russo, V. *et al.* Kinetic study of Amberlite IR120 catalyzed acid esterification of levulinic acid with ethanol: From batch to continuous operation. *Chemical Engineering Journal* **401**, 126126 (2020).

[34]Hofmann, H. Kinetic Data Analysis and Parameter Estimation. in *Chemical Reactor Design and Technology: Overview of the New Developments of Energy and Petrochemical Reactor Technologies. Projections for the 90's* (ed. de Lasa, H. I.) 69–105 (Springer Netherlands, 1986). doi:10.1007/978-94-009-4400-8_4.